1-1-2014

Predicting Flank Margin Cave Collapse in the Bahamas

Orry Patrick Lawrence

Predicting flank margin cave collapse in The Bahamas

By

Orry Lawrence

A Thesis
Submitted to the Faculty of
Mississippi State University
in Partial Fulfillment of the Requirements
for the Degree of Master of Science
in Geosciences
in the Department of Geosciences

Mississippi State, Mississippi

May 2014

Predicting flank margin cave collapse in The Bahamas

By

Orry Lawrence

Approved:

_____

John E. Mylroie
(Major Professor)

_____

John C. Rogers
(Committee Member)

_____

William H. Cooke III
(Committee Member)

_____

Michael E. Brown
(Graduate Coordinator)

_____

R. Gregory Dunaway
Professor and Dean
College of Arts & Sciences

Name: Orry Lawrence

Date of Degree: May 16, 2014

Institution: Mississippi State University

Major Field: Geosciences

Major Professor: John E. Mylroie

Title of Study: Predicting flank margin cave collapse in The Bahamas

Pages in Study: 83

Candidate for Degree of Master of Science

Sinkhole collapse is a common karst land-use risk around the world. In the Bahamas cover-collapse sinkholes do not exist because soil cover is thin; almost all collapse is due to cave ceiling failure. The most common cave types in the Bahamas are flank margin caves and banana holes. Flank margin caves have three entrance types: dissolution pit, side breach, or ceiling collapse. Both side breach and ceiling collapse are the result of mass erosional forces; pits by focused dissolution. It was previously proposed that slope was a controlling factor in Bahamian cave collapse. This study demonstrated that 7.5 minute topographic maps cannot resolve slopes accurately enough to predict potential collapse locations. Field surveys with 1 m contours allowed for a more concise slope range in which each entrance type preferentially occurred; collapse breaches and pits were common on gentle slopes and side breaches on steep slopes.

DEDICATION

I dedicate this study to Dr. John Mylroie for taking me on as his ninth consecutive graduate student, during the second semester of my graduate program, knowing that my last semester would be during his sabbatical. Dr. Mylroie's door was always open; he was dedicated to his students. It was a great pleasure working with "Doc", as I often called him. If it wasn't for Doc, I'm not sure I would have ever pursued a Master's Degree in Geology. His geology classes, taken as electives during my undergraduate GIS studies, intrigued me and inspired me to further my education. As well as being an excellent mentor, Dr. Mylroie was a great teacher, field-guide, and friend. Thanks doc.

ACKNOWLEDGEMENTS

First and foremost, I would like to give a big thanks to my parents. Thank you mom and dad for supporting me through everything, no matter what.

Thanks to Dr. Bill Cooke and Dr. John Rodgers for being on my committee and providing me with direction when needed. All of my colleagues in the department were great to work with and for that, I am grateful.

This project would not have been possible if it was not for Mr. Mike Lace and The Coastal Cave Survey; Mike supplied many gps locations and cave maps from various projects throughout The Bahamas. The Erwin-Russell Geology Endowment Fund provided funding to purchase the needed topographic map sheets.

Finally yet importantly, thanks to all my friends and family that have listened to me explain over and over again what it is that I have been studying. Regardless of whether they understood or not, they shook their head, said “interesting”, and told me that they believed in me.

TABLE OF CONTENTS

LIST OF TABLES

LIST OF FIGURES

CHAPTER I

INTRODUCTION

Cave roof-collapse is a land-use hazard that has long been of concern in the carbonate island setting, but field reconnaissance costs and difficulties have left much unanswered about cave roof-collapse risk. Caves and karst landscapes are recognized as a geologic hazard (White, 1988), including the special issue of islands (Wilson et al., 1995). Flank margin caves (Fig 1.1), which form by dissolution at the margin of the freshwater lens, are a major type of cave in carbonate islands. Flank margin caves commonly have portions that have collapsed (Fig 1.2), as well as areas where the roof is thin and prone to collapse. Banana holes (Fig 1.3), typically found in progradational strand plains, are small, immature flank margin caves with thin roofs that were abandoned during formation (Ho et al., 2013). Banana holes are thought to pose the greatest potential collapse hazard (in terms of frequency) due to their location beneath the relatively level terrace where most development occurs (Wilson et al., 1995). Because flank margin caves form near the flank of the enclosing landmass near the saltwater contact, and banana holes form in progradational strand plains, their general locations are relatively easy to predict. Flank margin caves, as well as banana holes, form as entranceless caves that cannot be observed from the surface until it is breached by hill retreat, roof collapse, or a pit intersection. Remote sensing and GIS technology provide venues by which spatial research on cave roof-collapse can be conducted (e.g. Ho et al.,

2013). The slope of the overlying topography is the only parameter that can be viewed remotely in efforts to infer what is happening beneath the surface. The slope would have an effect of roof thickness, leading to risk of collapse. The problem is that highly accurate satellite data are not available for this study area. The resolution of the topographic data will affect the possibility to calculate roof thickness and in turn diminish the ability to predict flank margin cave collapse.

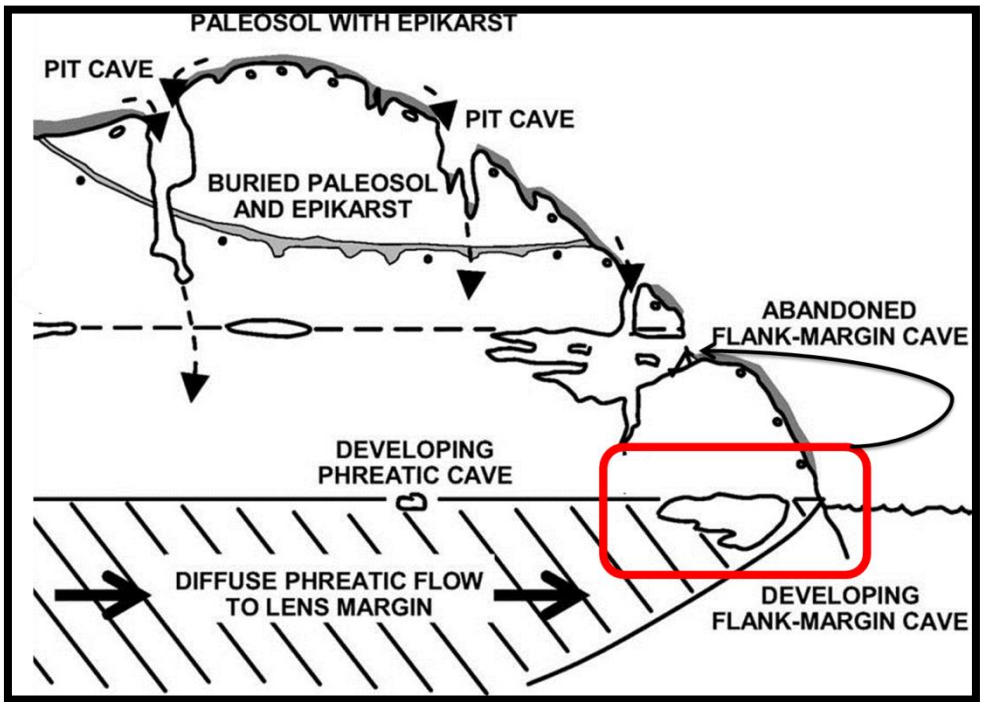

Figure 1.1 The margin of the freshwater lens is boxed in red showing where flank margin caves develop, due to the mixing of fresh and marine waters.

Figure 1.2 Flank margin cave demonstrating collapse in the Bahamas.

Figure 1.3 A banana hole in the Bahamas showing the result of bedrock roof collapse.

Flank margin caves differ from continental stream caves and sinkholes. Since the 1970's, the development of a comprehensive conceptual model for carbonate island karst has been under construction. After nearly a decade of field work, it was discovered that the continental interior stream-cave model was not functioning in the island setting (Mylroie and Mylroie, 2007). Over the years, advancements in the karst model have changed the way scientists identify specific karst features on islands. The Carbonate Island Karst Model (CIKM) was developed and validated via extensive fieldwork that included surveying and mapping each cave's location and extended profile (Jenson et al., 2006). Cave maps with detailed surveys were created for caves on many islands throughout the Bahamas over the past 38 years. Though the rationale behind the search for caves has not been to predict cave roof-collapse, years of data from the development of the CIKM, funded primarily by petroleum-influenced research, can now be used to assist in dealing with a potentially dangerous land-use hazard. The CIKM explains that the caves on many of these islands are not conduits, but rather mixing chambers - lacking evidence of turbulent flow (Mylroie and Mylroie, 2007). Vacher and Mylroie (2002, p. 183) differentiated "island karst" from "karst on islands" by explaining that "island karst" are those features which formed under the influence of the CIKM rather than the typical continental interior stream-cave model; "karst on islands" represents karst behavior similar to that seen on continents, commonly in large island interiors. The CIKM led to much advancement in karst related research that was previously difficult due to the lack of understanding of "island karst".

Can cave location along with the slope of the overlying topography address cave roof-collapse potential? The goal of this research is to establish a set of protocols to

assess cave roof-collapse risk for flank margin caves in the Bahamas. More specifically, the objective is to determine whether the 1972 Bahamas Lands and Surveys 7.5-minute topographic quadrangle map sheets have the resolution necessary to predict flank margin cave collapse. Can the distal slope of the overlying dune be used to predict where bedrock is suspected to be the thinnest? Roof thickness and maximum chamber width are the two factors that cause collapse in caves. Neither of the two factors that lead to collapse can be viewed from the surface. Since the slope of the topography can be remotely sensed/calculated, this project will test to see if the slope can be used as a proxy for roof thickness. This research is important to the literature because up to this point, there is no way to predict flank margin cave roof collapse. Finding a way to predict flank margin cave collapse would be a huge step in land development practices in the Bahamas (as well as other carbonate islands and coastlines).

CHAPTER II

LITERATURE REVIEW

Study Area

Located off the SE coast of Florida, the Bahamas make up a 1000 km portion of a NW-SE trending archipelago. Starting in the NW (27° 30' N, 79 10' W), the islands are positioned on large carbonate banks, but the farther SE islands are on much smaller, isolated banks, often not much bigger than the island itself (Fig 2.1). Between the banks are deep troughs in excess of 3000 m depth. The archipelago terminates in the SE with the Turks and Caicos Islands and the Silver and Navidad Banks, a separate political entity from the Bahamas (19° 50' N, 68°42'W). Made up of 29 major landmasses (islands), 661 cays (pronounced "keys", minor islands), and 2387 rocks (Albury, 1975), the Bahamas cover 300,000 km^2 (Meyerhoff and Hatten, 1974). At the current sea level position, 136,000 km^2 is shallow bank and 11,400 km^2 exists as land above sea level (Meyerhoff and Hatten, 1974). Sea level change can greatly affect the size of the Bahamian islands; with a 10-meter drop in sea level, the banks would be exposed causing the island to increase more than 10 times in size. The current sea level, if referenced from the Quaternary sea-level curve of the past 450 thousand years presented in Fig 2.2, is not the norm, yet more the exception. The Bahamas have been in a sea-level lowstand condition 85 – 90 percent of the past 450,000 years, meaning the banks were exposed (Mylroie and Carew, 2013). Sea level was at its highest and lowest points respectively, - 125 m

(25,000 - 19,000 ka) and +6 m (124,000-115,000 ka) (Mylroie and Mylroie, 2013a). Glacio-eustatic sea-level changes during the Quaternary alternately flooded and exposed the Bahamian banks, therefore causing cycles of deposition and dissolution, respectively. Carbonate deposition is only significant when platforms are flooded; the platforms have been flooded <15% of the past 450 ka (Mylroie and Carew, 2013). Deposition has resulted in a minimum sediment thickness of 5.4 km (Meyerhoff and Hatten, 1974) and up to 10 km (Uchupi et al., 1971) since the late Cretaceous. The previous sea-level highstand (MIS 5e ~ 120 ka) resulted in the surface being dominated by eolianites (fossilized carbonate sand dunes) and subtidal faces (including fossil reefs); above 8 m, the surface is expressed solely as eolianites (Mylroie and Mylroie, 2013a). Subsidence of 1-2 m per 100,000 years (Carew and Mylroie, 1995) due to isostacy results in rocks at the surface being less than a couple 100,000 years old , i.e., as the island subsides, beach and eolian processes build/deposit new dunes on top. Given the Bahamas are tectonically stable yet steadily subsiding, the only explanation for cave formations at +2 to +6 m above modern sea level is a previous glacioeustatic sea-level highstand. Therefore, any cave above sea level today had to form when sea level was higher, but also within recent enough history that it would not have subsided below sea level today. Karst features that formed during the Marine Isotope Substage 5e (MIS 5e) sea-level highstand would only have subsided approximately 1-2 m corresponding to the amount of time that has passed; remnant features from the past sea-level highstands such as MIS 9 or 11 would have subsided to or beneath current sea level. This only leaves the sea-level highstand MIS 5e (124-115 ka) to have raised the freshwater lens and formed the caves observed at +2 to +6m today (Mylroie and Mylroie, 2013a).

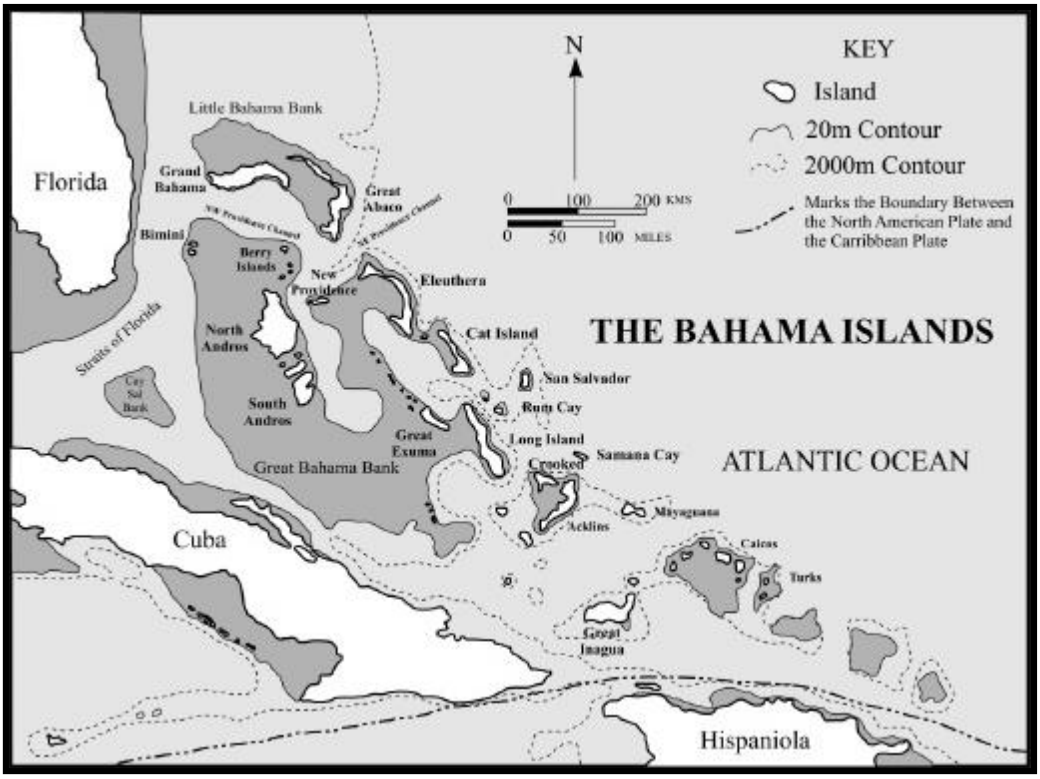

Figure 2.1 Map of the Bahamian archipelago showing the size of the shallow banks in dark grey and land above sea level in white. From Mylroie and Mylroie (2013a).

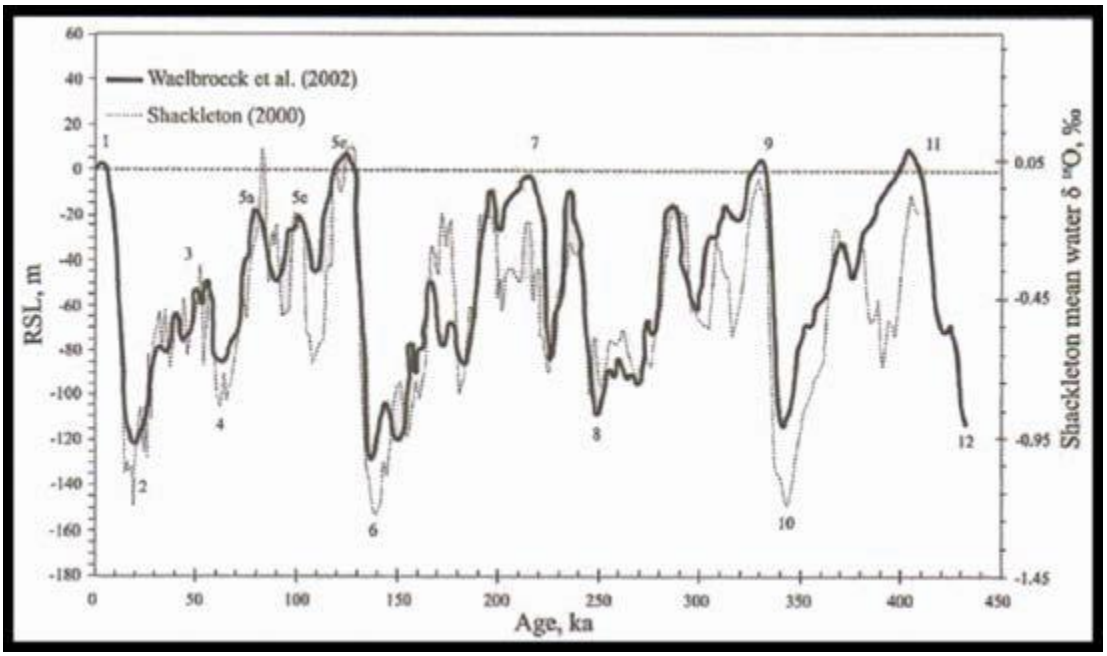

Figure 2.2 Sea level curve of the past 450 ka; note that nearly 85% of the past 450 ka has been spent below modern sea level. From Lascu (2005).

The processes including subsidence, lack of uplift, and continued deposition results in carbonates at the surface being diagenetically immature or eogenic. Choquette and Pray (1970, p. 215) described the maturation of limestone and broke them into three classes by the postdepostional evolution of carbonate porosity: eogenetic, mesogenetic, and telogenetic.

1. Eogenetic – "the time of early burial"
2. Mesogenetic – "the time of deeper burial"
3. Telogenetic – "the late stage associated with erosion of long buries carbonates"

Vacher and Mylroie (2002, p. 183) went on to define *eogenetic karst* as, "the land surface evolving on, and the pore system developing in, rocks undergoing eogenetic,

meteoric diagenesis." Other terms including *telogenetic karst*, "the karst developed on and within ancient rocks that are exposed after the porosity reduction of burial diagenesis", were created at this time. While karst can form in the mesogenetic environment, they would have to move into the telogenetic environment to be observed. The Bahamas being tectonically stable prohibits telogenic limestones and/or karst features from being present, therefore the karst and caves in the Bahamas are considered eogenetic in nature.

Geology of The Bahamas

The stratigraphy of the Bahamas is relatively simple; individual packages are marked by each sea-level highstand, and separated by erosional unconformities (often marked with a terra-rossa paleosol), indicative of a sea-level lowstand. There is no terrigeneous sediment present on the Bahamian banks because strong ocean currents isolate the banks from continental influence (Mylroie and Mylroie, 2013a); insolubles arrive as atmospheric dust. With ~ 100 percent carbonate composition and all exposed rocks only a couple 100,000 years in age, (Mayaguana is an exception that does not apply here), there are only three geologic formations to review (Mylroie and Carew, 2013). These units are as follows from oldest to youngest: the Owl's Hole Formation, the Grotto Beach Formation, and the Rice Bay Formation (Fig 2.3).

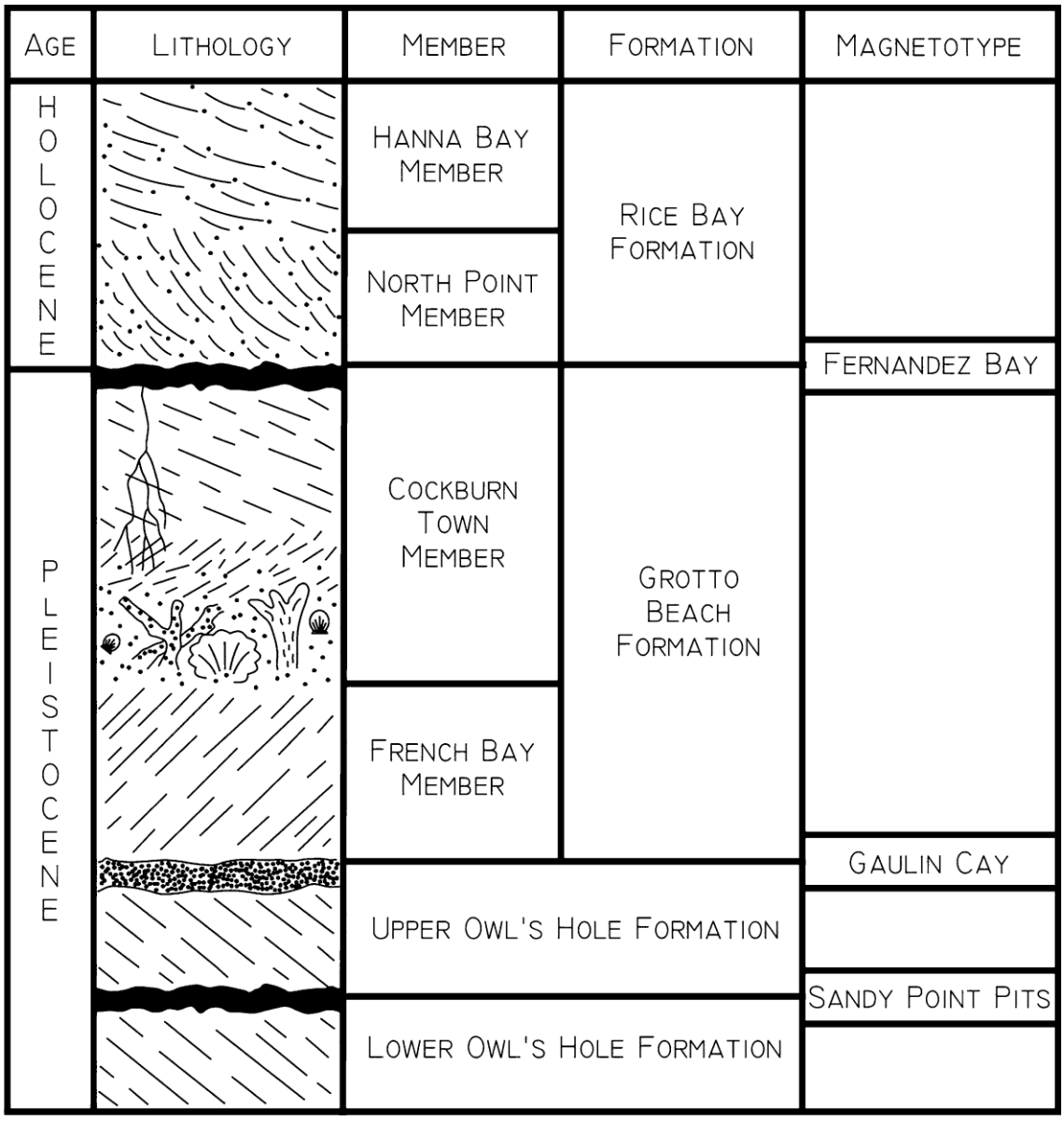

Figure 2.3 Simplified stratigraphy of the Bahamas, from Mylroie and Carew (2013). For a more detailed stratigraphy, see Kindler et al. (2010)

Owls Hole Formation

The Owl's Hole Formation, comprised entirely of eolianites, is the oldest formation expressed at the surface on all Bahamian islands, except on Mayaguana (Mylroie and Carew, 2013). This formation has multiple paleosols indicating platform

emergence during glacio-eustatic sea-level lowstands, as well as multiple carbonate deposition events as the platform was flooded and exposed alternately (Mylroie and Carew, 2013). Carbonate rocks from the Miocene through early Pleistocene have been described on Mayaguana (Kindler et al., 2010), most likely exposed by a slight platform tilt to the south, but there is no need to break down the Owl's Hole Formation any further since no other surface expression of these older rocks is found elsewhere in the Bahamas. Note that there would be older formations at depth but are not discussed as they have subsided and will not be of any diagnostic value. There are many dry caves in the Owl's Hole Formation. There are no subtidal units known in the Owl's Hole Formation as they too have subsided below modern sea level.

Grotto Beach Formation

Separated by a terra-rossa paleosol or erosional unconformity, the Grotto Beach Formation overlies the Owl's Hole Formation. The Grotto Beach Formation developed during the last interglacial, Marine Isotope Substage 5e (MIS 5e), 124,000 to 115,000 years ago (Mylroie and Carew, 2013). This span of only 9,000 years resulted in the deposition of the entire Grotto Beach Formation, as well as the phreatic karst features that subsequently formed within the rock. Once again, the time constraints in which these caves form is remarkable. Given that sea level was +6m during the last interglacial, subtidal facies (fossil reef or lagoons) are found above sea level in the Grotto Beach Formation. This formation is broken into two members, the French Bay Member represents a transgressive phase (when sea level was rising), and the Cockburn Town Member represents a stillstand and a regressive phase (when sea level was falling). These two members are distinctly different, but ooids are a diagnostic feature for both

members of the Grotto Beach Formation (ooids are rare in the Owl's Hole Formation on San Salvador). A wave cut bench is indicative of a transgressive cycle; as sea level rises, the dunes are attacked by wave action. Shallow water over a wave cut bench makes coral growth prominent. The Cockburn Town Member, younger and more complex, is made up of subtidal and intertidal facies overlain by stillstand and regressive dunes. Subtidal facies above modern sea level help easily identify the Cockburn Town Member in the field.

Stillstand episodes during the Cockburn Town Member highstand allowed for progradational growth of strandplains (Fig 2.4) along coastlines. Progradation of the shoreline results in a beach-ridge system with dune ridges and swales parallel to the coastline. Strandplains build outwards during stillstand phases as sediments pile up in the foreshore environment until reaching wave base and being pushed onshore forming new land. This progradational process allows banana holes to form as the freshwater lens moves into new land. Dissolution is always occurring at the freshwater/saltwater contact, but when the freshwater lens advances seaward into new land and abandons the previous freshwater lens position, immature flank margin caves are formed and in turn, abandoned (Fig 2.5). Banana holes found in the progradational strand plains developed in this manner. All caves +6m above modern sea level are from the Cockburn Town Member time (124-115 ka), the last time sea level was above modern in the Bahamas; the caves are found in both Grotto Beach and Owl's Formation rocks.

Figure 2.4 Sandy Hook is a good example of a Holocene progradational strandplain on the south end of San Salvador.

Notice the parallel dune ridges along the easternmost portion of the image. This area is expected to hold many developing immature flank margin caves, referred to as banana holes. From Mylroie et al. (2012).

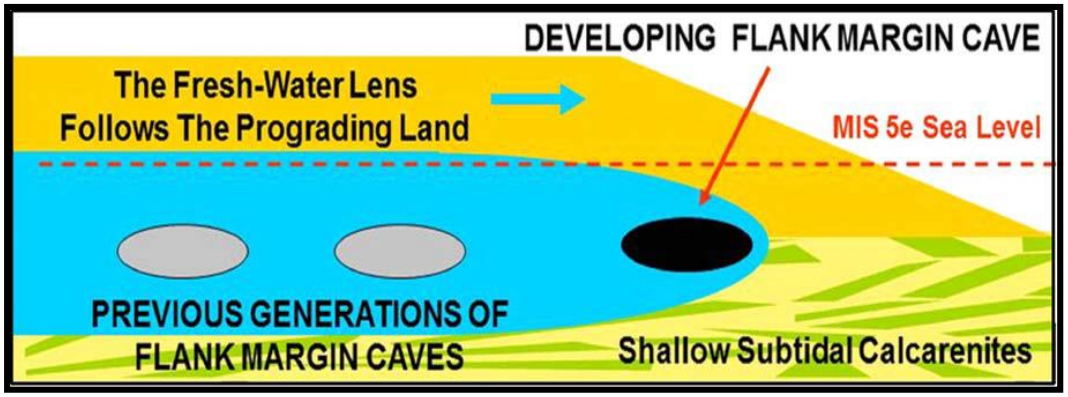

Figure 2.5 Diagram representing the formation of banana holes in progradational strandplains. From Mylroie et al (2012).

Rice Bay Formation

The Holocene Rice Bay Formation is the youngest unit of rock found in the Bahamas, and is separated from the Grotto Beach Formation by a terra-rossa paleosol or other erosional surface. It is made up of the North Point Member (transgressive phase) where eolian beds dip below modern sea level, and the Hannah Bay Member (stillstand phase), where eolian beds grade into beach facies at modern sea level. The Rice Bay Formation is entirely eolianites, with beach rock in the Hanna Bay Member. Because of their very young age, rocks of the Rice Bay Formation do not have a terra-rossa paleosol covering them, and do not have karst caves expressed at the surface today. This is not to say that flank margin caves have not formed in the Rice Bay Formation, just that cliff retreat has not breached these caves creating an entrance, which would be at modern sea level. While caves are not expressed at the surface, small dissolution caves throughout modern strandplains are anticipated due to the stillstand phases of the Hanna Bay Member.

Karst

Karst is widely known as, "the landscape created by dissolution and solution on the soluble rock, such as limestone, halite, and gypsum" (Ford and Williams, 2007, p. 1). According to White (1988), in 1967 Gvozdetskii estimated that 20 percent of the earth's land surface qualifies as karst. Mylroie (1995) goes on to say karst processes dominate carbonate islands. We will adhere to White's (1988, p. 4) definition of karst for this paper, "all landforms produced by the solution process-regardless of scale, surface expression, or rock type".

Karst Classification

In the literature today, there are multiple ways that cave and karst features are characterized. Palmer (1991) described karst in a new way; he characterized karst by the mode of recharge to the soluble rock. Epigene karst, the karst typically described in the literature, refers to karst that formed by meteoric recharge (i.e., the continental interior stream-cave model).

As stated by Mylroie and Mylroie (2007), after nearly a decade of fieldwork on islands, it was discovered that the continental interior stream-cave model was not functioning in the island setting, and it was then that Palmer coined the two terms, epigene and hypogene. Palmer (1991) described epigene karst as karst formed by the movement of water across the surface and from vadose into phreatic conditions, which increases the dissolution potential of the solution at depth by increasing the amount of carbonic acid from the atmosphere and soil. Hypogene caves dissolution potential is driven by carbonic acid and hydrosulfuric acid, as well as a variety of other possibilities including: where water becomes solutionally aggressive because of mixing, oxidation of

H_2S, or a drop in temperature (Palmer, 1991). Hypogene caves form in phreatic conditions, decoupled from the surface hydrology, and gain their dissolution potential from mixing waters of different chemistries (Palmer, 1991). Flank margin caves are thought to be hypogene in nature because the aggressive solutions origin is below the surface, and the caves are not directly coupled to surface hydrology.

There is debate in the karst community today whether flank margin caves are actually a subtype of hypogene cave or whether flank margin caves should be considered "island karst" (e.g. Klimchouk, 2007). Vacher and Mylroie (2002, p. 183) differentiated "island karst" from "karst on islands" by explaining that "island karst" are those features which formed under the influence of the CIKM rather than the typical continental interior stream-cave model. "Karst on islands" represents karst behavior similar to that seen on continents, commonly in large island interiors. A recent conference on hypogene caves (Klimchouk et al., 2014) did not reach a conclusion about flank margin caves, and many workers place them in a category called "coastal caves".

For this study, the choice is, "Island karst caves" are hypogenic in nature and form under the influence of the CIKM; "Karst on islands" are epigenic in nature and form under the influence of the continental interior stream-cave model. There is no part of the definition of hypogene caves that flank margin caves do not conform to, therefore it should stand that flank margin caves are a subtype of hypogene cave.

Flank margin cave model

The flank margin cave model explains the dissolution process in coastal carbonates as the result of the following three phenomena that occur at the lens margin (Mylroie and Mylroie, 2007).

1. Mixing of freshwater and seawater result in a solution with renewed dissolution potential.
2. The decreasing cross sectional area of the lens margin increases flow velocity, speeding up dissolution by getting the reactants in and products out quickly (i.e. as the rock is dissolved chemically, it is also transported away).
3. Organics collect at density interfaces near the top and bottom of the freshwater lens. The increased CO_2 from oxidation increases dissolution. With extremely high organic loading, anoxic conditions can allow H_2S and other acidic solutions to further drive dissolution.

The Carbonate Island Karst Model (CIKM)

The Bahamas were the host site for the development of an island karst model, which began in the mid 1970's, first with the flank margin cave model and then the CIKM. The CIKM was initiated when the flank margin cave model was extended to more and more complex islands (Mylroie and Mylroie, 2007). The CIKM consists first of the flank margin cave model plus the increasingly complex factors that add to the equation such as tectonics, sea-level change, and non-carbonate rocks. The CIKM summarizes the principles that control the development of karst on carbonate islands in an attempt to characterize the levels of complexity found within carbonate islands. The principles of the CIKM have been updated since first outlined by Mylroie and Vacher (1999) as new studies have been completed (e.g. Mylroie, 2013).

The principles of the CIKM, from Mylroie (2013), are:

1.) The mixing of freshwater and saltwater results in an aggressive fluid in respect to $CaCO_3$ (Fig 2.6). Two fluids, both which are saturated with respect to $CaCO_3$,

when combined, will have a renewed dissolution potential. These mixing zones occur in two areas, at the vadose/phreatic interface, as well as the contact of the bottom of the freshwater lens with the seawater below (Fig 2.7). The top and bottom of the freshwater lens create a density interface, resulting in the collection of organics at these density interfaces. The oxidation of these organics increases levels of CO_2, further driving the dissolution process. These two mixing zones are superimposed near the margin of the freshwater lens, resulting in the maximum amount of dissolution at the lens margin (Fig 2.7); exceptional organic loading can create anoxic conditions and production of exotic acids such as H_2S. In essence, the first part of the CIKM is the flank margin cave model.

2.) Sea-level change moves the position of the freshwater lens. As the freshwater lens moves up and down, this mixing zone follows creating dissolution features at the new location of the mixing zone. Sea level has moved up and down 100 m or more throughout the Quaternary as a result of glacioeustasy. Tectonics can move local sea level independent of glacioeustasy. Overprinting of features developed during different glacio-eustatic events can occur by local tectonic movement, sediment compaction, and isostatic adjustment.

3.) Many continental carbonates around the world are millions of years old, but the carbonates found on almost all tropical islands are young, eogenetic rocks. The CIKM is a model developed to deal specifically with *eogenetic* carbonate rock that has never been buried below the zone of meteoric diagenesis. Note that *telogenic* rocks, those that have been buried before, do occur on carbonate islands

and this model can be used for those areas, especially if conditions are favorable (see Mylroie and Mylroie, 2013b).

4.) There are four classifications of islands: Simple, Carbonate-Cover, Composite, and Complex. These classifications are based on their respective carbonate vs non-carbonate geology, and sea level position (Fig 2.8). While not all islands fit into a single classification scheme, these classifications are idealized boundary conditions that can be applied to portions of islands when necessary.

I. Simple Island – Fig 2.8 A

- Only carbonate rocks at the surface
- Only carbonate rocks in range of the freshwater lens
- Autogenic catchment

II. Carbonate-cover Island – Fig 2.8 B

- Only carbonate rocks at the surface
- But consists of non-carbonate rock underneath which can partition the freshwater lens
- Conduit cave systems can form at the contact of the carbonate and non-carbonate rocks
- Autogenic catchment

III. Composite Island – Fig 2.8 C

- Both carbonate and non-carbonate rocks at the surface

- Conduit cave systems can form at the contact of the carbonate and non-carbonate rocks
- Autogenic and allogenic catchment (allogenic due to non-carbonate rock)

IV. Complex Island – Fig 2.8 D

- Carbonate and non-carbonate rocks are complexly mixed together due to

  depositional relationships and/or faulting
- The freshwater lens can be perched, isolated, or confined
- Autogenic and allogenic catchment (allogenic due to non-carbonate rock)

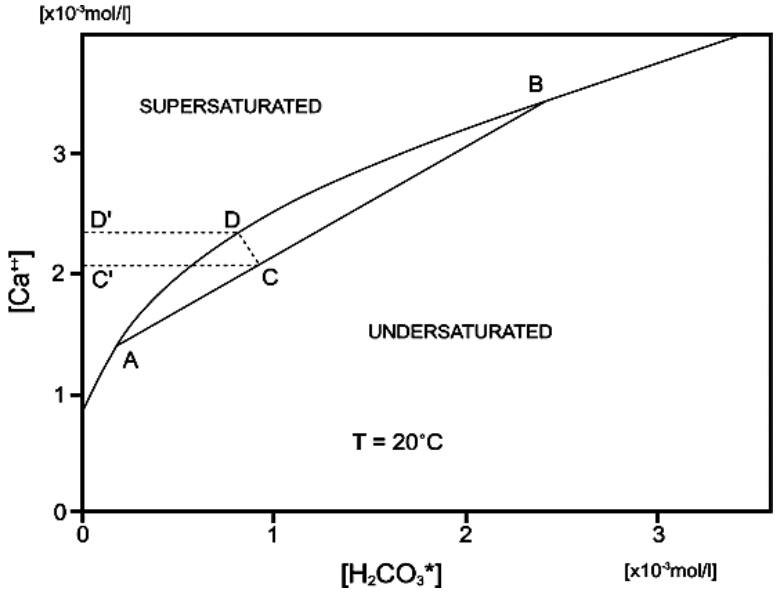

Figure 2.6 Saturation curve for $CaCO_3$. From Dreybrodt (2000).

Mylroie and Mylroie (2007, p. 60) explains:
"Because the saturation curve for CaCO3 is convex upward, waters saturated at two different initial conditions, as at A and B in the figure, when mixed create a water body, C, that is beneath the saturation curve, and so is unsaturated. This water body now has renewed dissolutional potential and will dissolve CaCO3 until it again reaches the saturation curve at D."

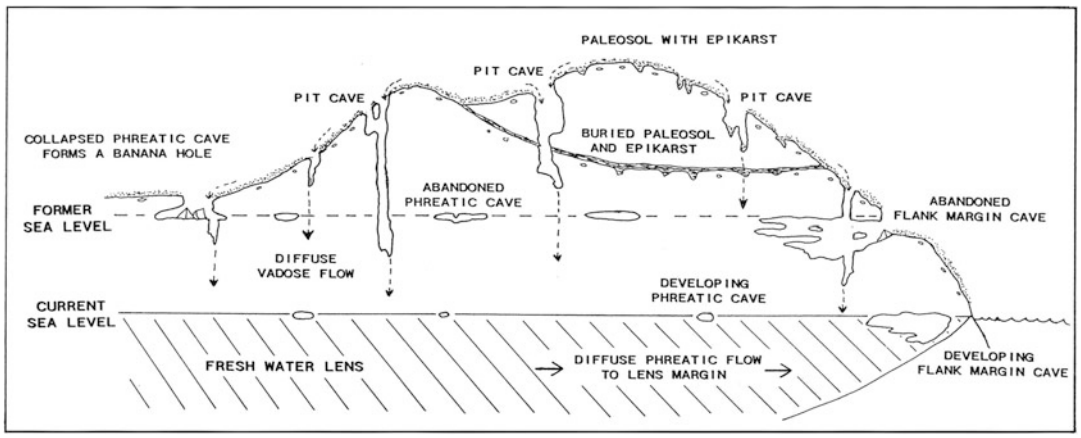

Figure 2.7 The freshwater lens within the carbonate rock mixes with seawater from below to create flank margin caves at the margin of the freshwater lens under the flank of the dune.

This diagram also illustrates most of the karst features found on the islands except blue holes. From Mylroie and Mylroie (2013a)

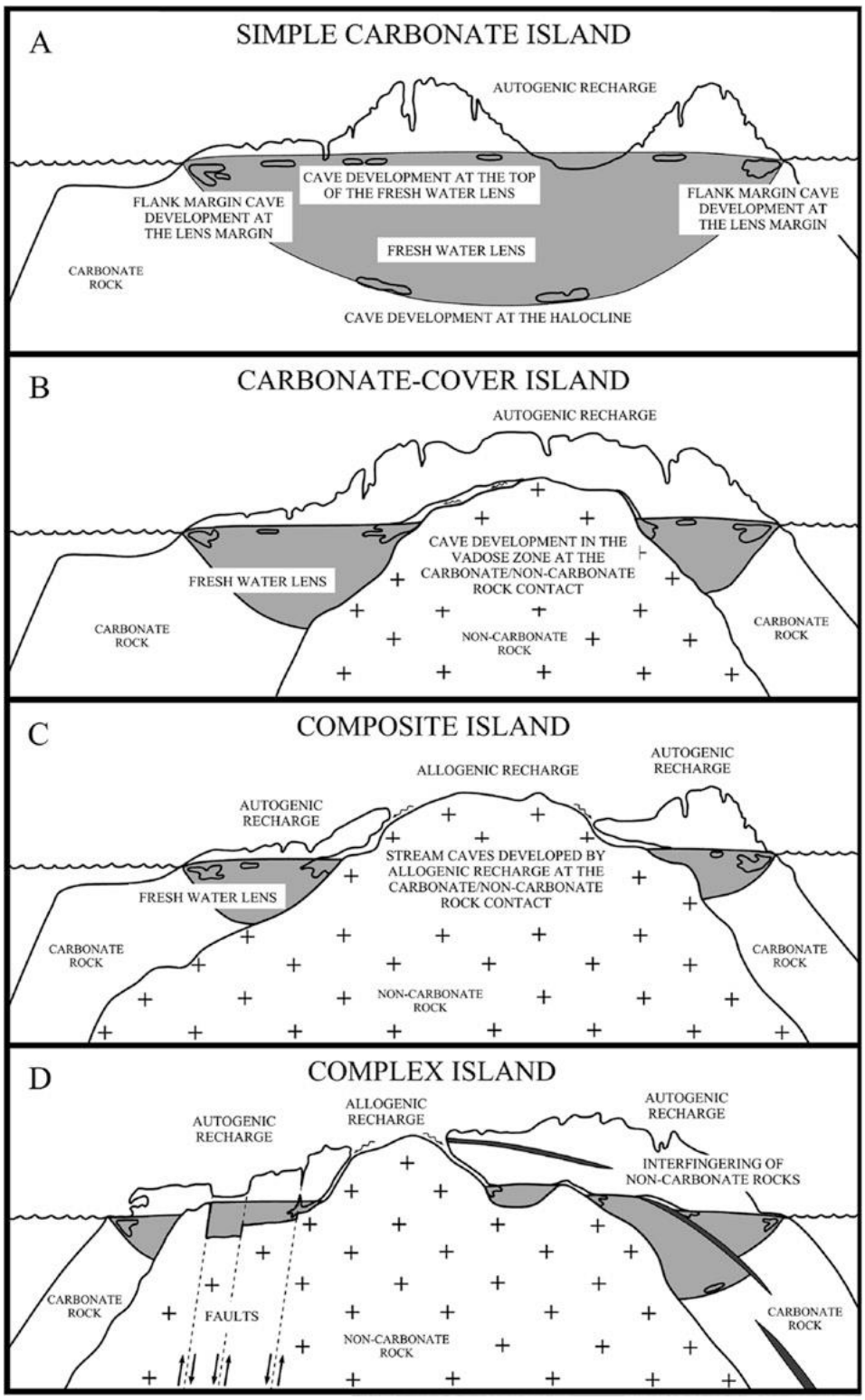

Figure 2.8 The four classifications of islands addressed in the CIKM.

The Bahamas are classified as a type (A), simple carbonate island. From Mylroie (2013).

Impact of karst on carbonate islands

Caves and karst landscapes have much to offer people from all walks of life including nature enthusiasts who enjoy dramatic landscapes and adventures, as well as scientists who study caves, their environments, and their geomorphologic processes for various reasons (White, 1988). Unfortunately, along with the natural beauty that many karst features provide, there are many land-use hazards that must be considered. First, karst land-use hazards will be addressed from a global perspective and then more specifically from an island karst perspective.

Karst terrains affect two important factors of land development:

1. Water resources
2. Land stability

Water Resources

Karst landscapes and the dissolution pathways that form within the rock throughout the subsurface bring forth two issues. The immediate infiltration of surface water deems both water quantity and water quality vulnerable in the carbonate setting (not to mention soil loss). White (1988, p. 380) states, “Water management in the karst is a special problem as is, for example, water management in deserts or on small islands”. Water is difficult to obtain due to a combination of things such as the absence of surface drainage, rapid infiltration, and internal runoff in karst terrains (White, 1988). Obtaining freshwater requires well extraction, but well siting and effective collection is difficult in limestone areas (Ford and Williams, 2007). With a limited water budget, contamination is critical. In a non-carbonate setting, water infiltrates through the soil, slowly being filtered and cleaned as it moves through the surface, but the direct fast flow connections to the

water table provided by dissolution pathways in limestone allow contaminants to travel further distances and to be a greater risk than once anticipated. Dye traces performed by Aley (1972) confirmed flow routes of 25 km to distant springs. White (1988) covers a variety of possible water contamination sources for karst freshwater including: dumps, hydrocarbon spills/leaks, floods, concentrated runoff (from road salt/parking lot/feedlot or barnyard), leaking tanks or pipes, industrial waste, organic chemicals, and saltwater intrusion. These contamination issues are more prevalent in karst hydrology than other settings due to the ability for these conduits to transmit water, unfiltered, over long distances, with turbulent flow, to unexpected destinations. The mixing chambers of the "island karst" features do not transmit water through conduits, but the danger of contamination is still critical.

Land Stability

Land stability issues in karst landscapes can be a nuisance to farm practices, yielding acres of worthless land (Ford and Williams, 2007). Mayan agricultural practices such as slash-and-burn (milpa) farming transformed the Yucatan Peninsula into a karst desert, as the soils were lost to the subsurface (Doehring and Butler, 1974). Cutter-and-pinnacle topography (Fig 2.9) at depth can result in differential compaction and foundation damage (White, 1988). White (1988) refers to Knight (1971) which said, "Karst lands are the bane of building construction". Limestone bedrock under a streambed can have solution conduits in excess of 100 meters in length near dams (Moneymaker, 1941). This suggests the channels may not support the dam if waters drain via conduit flow. Assessment of the channel bedrock must be performed when considering creating a reservoir in karst terrains.

Figure 2.9 This road cut shows cutter-and- pinnacle topography at depth (arrows), which allows for differential compaction if a structure is built on the land surface (i.e. compacting more on the right than on the left).

Modified from Lace and Mylroie (2013).

Karst landscapes vary in expression due to the geomorphological processes that formed the karst feature. Depending on geographical presentation, karst features may be interpreted as sinkholes, irregular rocky landscapes, shallow collapse features, blue holes, or underground caves, all of which pose different land-use hazards for water resources and land stability. Karst features are characterized by the geomorphological processes that sculpture them (White, 1988). Understanding the process and environment in which each feature occurs allows land management strategies to be adjusted for various feature types or terrains. While most karst research in the past has been conducted on the continents, the process and environment in which "island karst" form has not been previously understood and applied to land use management.

Breakdown

White (1988) discusses roof breakdown in the continental cave setting. There are two factors to consider when evaluating roof breakdown, beam thickness (roof thickness) and beam length (maximum chamber width). White goes on to explain that many island settings are more homogeneous than the continental setting, especially the carbonate islands. The beam thickness that White (1988) refers to is unit layers of overburden, i.e., each layer of homogeneous rock type. Beam thickness is especially important when there are alternating layers of rock, some rock units being stronger than others are due to differences in density and flexural strength (White, 1988). In the Bahamas, the carbonate is young and relatively homogeneous in nature from the surface to kilometers at depth (Meyerhoff and Hatten, 1974; Uchupi et al., 1971). Rather than referring to the overlying singular rock type as a beam, for the remainder of this paper, the beam thickness may be referred to as the roof thickness. Now, with a homogenous overburden, it is simpler to calculate the overhead roof strength. Whether it is a fixed beam or a cantilever, the density and flexural strength of the beam rock will be the same in all calculations. The fixed beam, the stronger of the two, is supported on both sides by beds above and below, while the cantilever beam is supported only on one side. The roof span or beam length, density, and flexural strength of the rock are used to calculate the critical thickness or the thickness in which the overburden must be to support the air-filled void. This study will focus in part on the critical thickness in which collapse occurs in carbonates.

Collapse Hazards

The common dictionary definition of collapse reads, “to fall down or inward suddenly; cave in” (American Heritage, 2003). Collapse poses perhaps the biggest threat

among the many land-use hazards of karst landscapes. There are two types of collapse hazards:

1. Cover-collapse
2. Cave roof-collapse

Cover-collapse

Cover-collapse sinkholes (Fig 2.10), formed by the washout of sediment overlying cavernous bedrock, are dangerous due to the unpredictable timing of collapse. Sinkholes form by processes termed, *epigenic*, receiving water from the surface and dissolving limestone as it makes its way to the water table (Palmer, 1991). Sinkholes and pit caves alike transmit water vertically through vadose fast flow routes. The collapse occurs after processes have created a void in the overlying sediments, which collapses instantaneously as illustrated in Fig 2.11. Pit caves (Fig 2.12) occur in locations where the carbonates are expressed at the surface (i.e., when there is not a thick soil layer available to create the soil arch). Continental stream caves, pit caves, and typical sinkholes formed by epigenic processes are not of real concern for the scope of this paper; therefore, cover collapse sinkholes and other epigenic karst features can be disregarded for the remainder of this paper. The Bahamas lack thick soils, or "cover", so large voids cannot be hosted with such a thin cover, and cover collapse therefore does not occur.

Figure 2.10 Sinkhole formed under a Chevrolet Corvette car museum in Kentucky.

When the collapse occurred , the cars fell into the cavity. Thankfully, the collapse occurred at night when no one was in the museum. (USA Today, 2014)

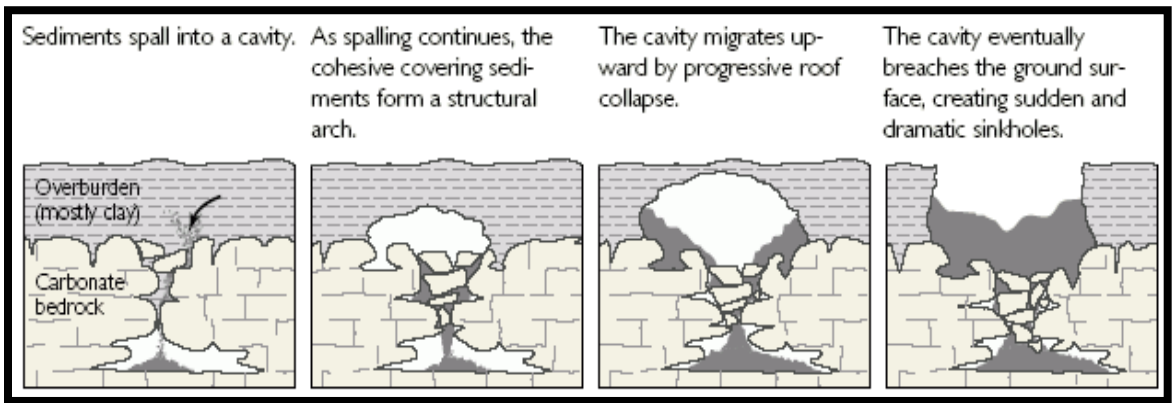

Figure 2.11 Cartoon diagram of how a cover-collapse sinkhole forms and collapses into the void at depth (USGS, 2013).

Figure 2.12 Pit caves, which form by epigenic processes, act as fast flow routes to the subsurface.

Cave roof collapse

Water resources and minor land stability issues seem dangerous enough, but collapse events (Fig 2.13) are often catastrophic and even fatal (e.g. Barbados, see Kambesis and Machel, 2013, p. 241-242). Cave roof collapse is associated with flank margin caves; a karst feature formed by processes decoupled from interactions with surface waters. As previously noted by Palmer (1991), flank margin caves are formed in phreatic conditions with mixing waters of different chemistries at the location of the island margin at the time of cave formation (sea-level change means that the location of

the margin of the freshwater lens then may not be the margin now). With sea level in a different position today than when these voids were created, it is important to locate flank margin caves before developing the land surface in order to mitigate the effects of cave roof collapse (Fig 2.14). The objective of this study requires the remainder of this thesis to specifically address the island karst cave roof-collapse issue and disregard all other land-use hazards associated with the karst environment.

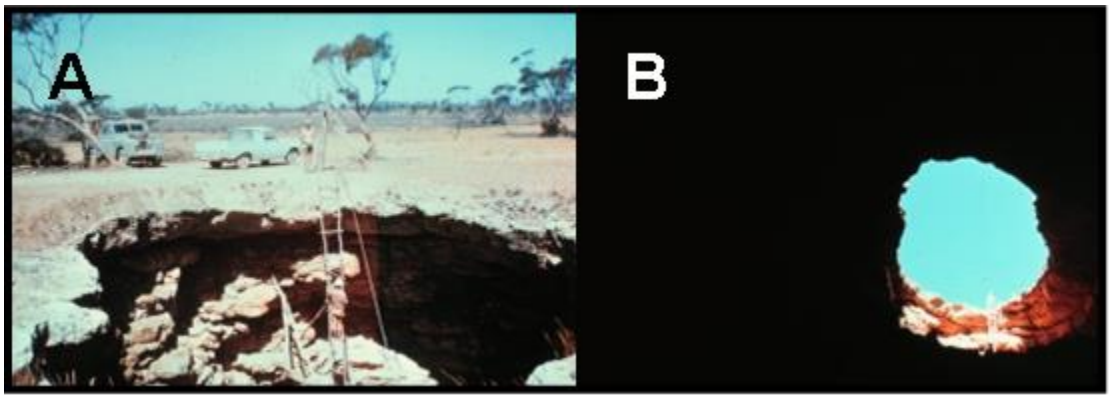

Figure 2.13 A) Collapse of a thin bedrock roof. B) A view from below, looking out of the hole in the roof.

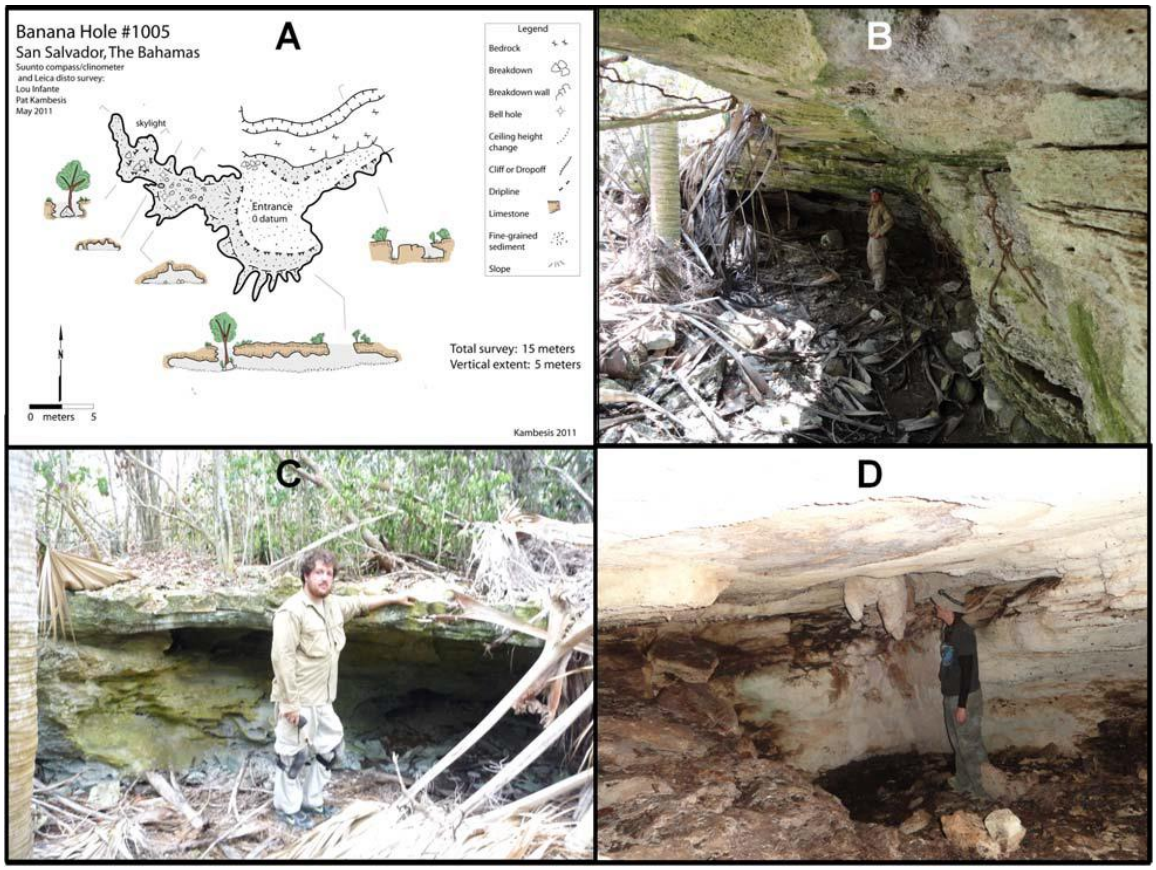

Figure 2.14 Images and map of banana holes from San Salvador Island, Bahamas.

A) Map of a partially collapsed banana hole. B) Large, partially collapsed banana hole; note the 2m of wall exposure (man for scale). C) Image of another partially collapsed banana hole; note the depth of the void is chest high on the man in the image. D) Banana hole chamber with intact roof. From Mylroie et al. (2012).

It has been suggested that dune slope could have a significant effect on the collapse of flank margin caves (Wilson et al., 1995; Ho et al., 2013). It was proposed that the distal slope of the overlying dune could render some insight for determining the overburden thickness of subsurface voids, and therefore their collapse potential. The problem with this approach is that the topographic maps that would be used to determine slope and infer bedrock thickness over potential flank margin caves may lack the contour resolution necessary to accurately display slope at the scale of the caves themselves. The

subtle variations in hillslope may not be recognized due to the 20 ft (6 m) contour resolution, limiting the predictive capabilities of derived slope as a proxy. An analysis of slope, as determined from topographic maps, coupled with maps of known caves, will be conducted to determine if those slopes are a predictor of cave collapse. The hypothesis to be tested is:

> *Topographic maps produced by the Bahamas Lands and Surveys Department are insufficient in resolution to be used as a predictor of flank margin cave collapse risk in The Bahamas*.

CHAPTER III

METHODS

The Bahamas are classified as a Simple Carbonate Island under the conditions of the CIKM. The Bahamas provide an ideal study area to develop a test model for hypogenic cave roof-collapse due to the islands' youth, relatively simple geology, and lack of tectonics. The majority of this research is based on cave data that has been archived over the past 38 years during the development of the Carbonate Island Karst Model (CIKM) (e.g. Mylroie and Mylroie, 2007). The work was conducted under a Bahamian government research permit issued to Dr. John Mylroie.

Data Collection

There are three types of data needed to complete this project: cave location data (GPS points, 15 m accuracy), cave maps, and topographic maps for the entire study area. The SRTM (Shuttle Radar Topography Mission) DEMs available from the US government have 90 m accuracy. The STRM DEMs provide less accuracy than 1972 topo maps, which have 20 ft (6 m) contours. For this reason, topographic maps from the Lands and Surveys Department of the Bahamas were used to obtain the slope overlying each cave. These topo maps have 20 ft (6 m) contour lines and allow the position of the cave to be plotted on the surface, as well as calculate the slope for that area. Some maps have

a 10 ft (3 m) contour line placed between the 20 ft (6 m) elevation and sea level in coastal areas, for better resolution of coasts.

Slope Analysis

First, the caves are positioned on the topographic map using GPS location data acquired from Dr. Mylroie (Dr. Mylroie is the Chief Scientist of the Coastal Cave Survey). Each cave's x-y location was loaded into Google Earth and then manually plotted onto each island's topographic map. The topographic map set for each island consisted of 2 to 28 sheets to cover the entire island and various cays surrounding each island. Cave maps and/or topographic maps were not available for every cave that had a GPS point; only the caves with GPS location, a detailed cave map, and the corresponding topographic map sheet were used in the study. Each cave was located on the topographic map, and the slope inputs (rise/run) were manually measured using calipers and the map scale. The slope inputs were then recorded in Microsoft Excel to populate rise and run columns. Next, using functions offered in Excel, the slope was derived by using the following formula: Slope=DEGREES (ATAN (rise/run)). By analyzing the slope of the flank of the dune, properly placing the cave and its vertical profile in relation to that slope, which sections demonstrate collapse and how thick the roof (overburden) is in those areas can be estimated.

Cave Entrances

The secondary analysis should aid in the prediction of cave collapse risk in potentially dangerous regions with unknown caves using a slope/collapse relationship. Some caves have many entrances and areas with collapse, while others may have a single

entry point with little to no evidence of collapse. When analyzing each cave map, each cave entrance was recorded in Excel and categorized by the following entrance types: side breach (cliff retreat), roof collapse, or pit intersection. The differentiation between collapse and pit intersection was subjective but used the following criteria: if the hole in the roof was small and no collapse breccia was noted on the floor of the cave, the entrance classification was assigned as a pit intersection. The total number of entrances was also recorded. The slope of the overlying topography was plotted against each of the three categories of entrances and the sum of the entrances in efforts to determine if a relationship between slope and entrance type exists. Subsequently, during analysis, side and collapse entrances were treated as a single entrance type (mass wasting), to differentiate them from the simple downward dissolution formation mechanism of pit entrances.

Unsupported Span (maximum chamber width)

The maximum chamber width was recorded to help determine the relationship between roof span and roof collapse. By documenting the maximum unsupported span, along with the overlying slope, it can be further demonstrated what effect slope has on roof thickness, that in turn allows collapse. For example, a cave with chamber size (x) and an overlying slope (z) does not demonstrate collapse, but another cave with equal chamber size (x) and lessor overlying slope (y) does demonstrate collapse. This approach reveals how chamber size, effects collapse potential when coupled with roof thickness. It is not believed that cave chamber size alone is the cause for collapse, as there are caves with huge chambers with very little to zero collapse. The cause for collapse is beam

thickness (roof thickness) coupled with the maximum unsupported span, neither of the two causes collapse by itself.

Data Analysis

The data collected will not have a normal distribution. The data will be presented by histograms as a nonparametic display to determine if there is a relationship between the cave entrances and cave chambers, and the slopes that surround them.

CHAPTER IV

RESULTS

A total of 107 caves across eight islands (consisting of over 70 topographic map sheets) were analyzed to determine if slopes calculated from topographic maps were predictive of the degree of flank margin cave collapse. Figures 4.1, 4.2, 4.2, 4.4, 4.5, 4.6, 4.7, 4.8, and 4.9 show the study area with the cave locations plotted into Google Earth using GPS data points. The full table of results for slope, entrance type/quantity, and maximum chamber width for each cave are shown in Appendix A.

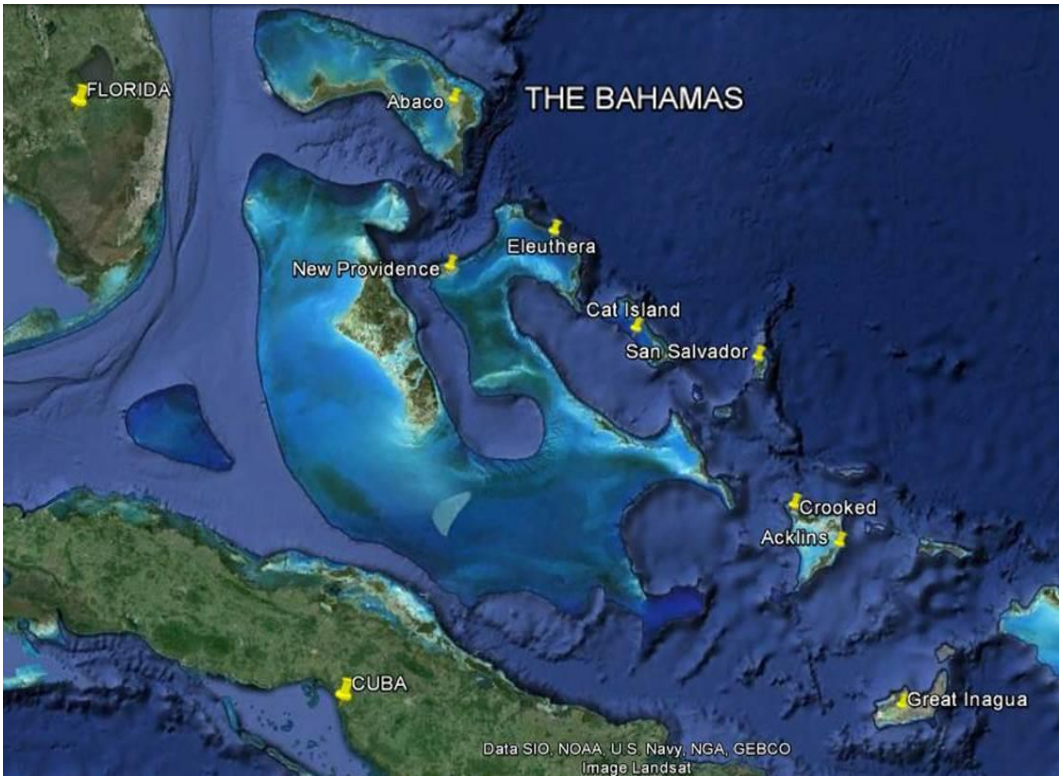

Figure 4.1 The study area with each island used in the topographic map analysis of The Bahamas labeled.

Other nearby political entities are also labeled for geographic reference. (Google Earth, 2014).

Figure 4.2 Caves used in the topographic map analysis plotted on Abaco Island (Google Earth, 2014).

Figure 4.3 Caves used in the topographic map analysis plotted on Acklins Island (Google Earth, 2014).

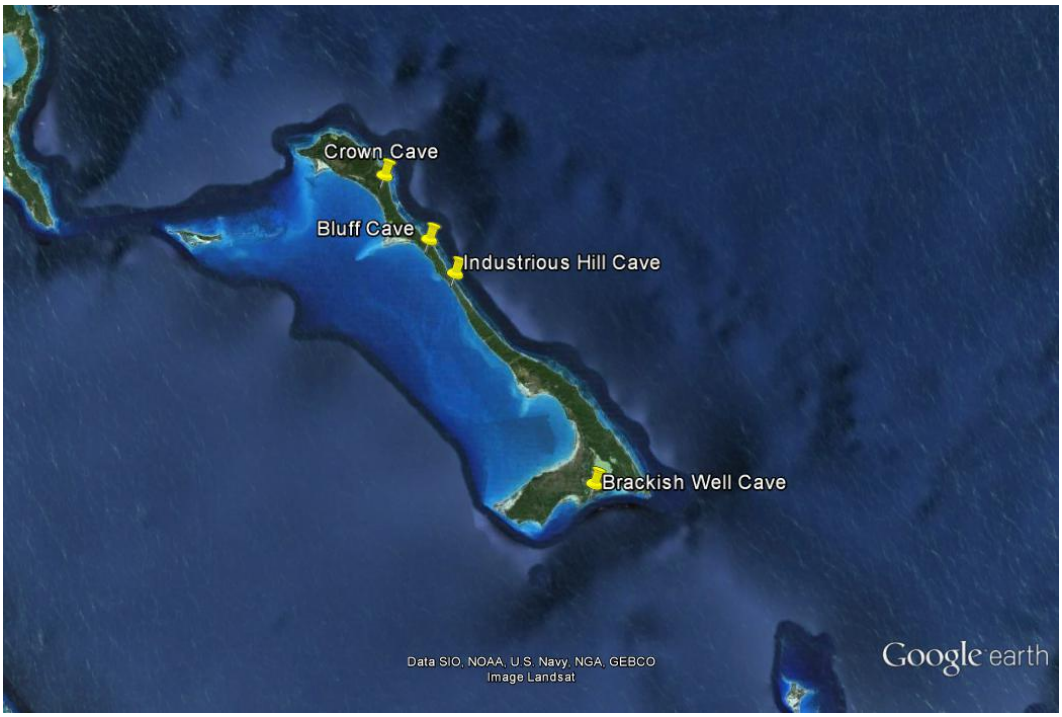

Figure 4.4 Caves used in the topographic map analysis plotted on Cat Island (Google Earth, 2014).

Figure 4.5 Caves used in the topographic map analysis plotted on Crooked Island (Google Earth, 2014).

Figure 4.6 Caves used in the topographic map analysis plotted on Eleuthera (Google Earth, 2014).

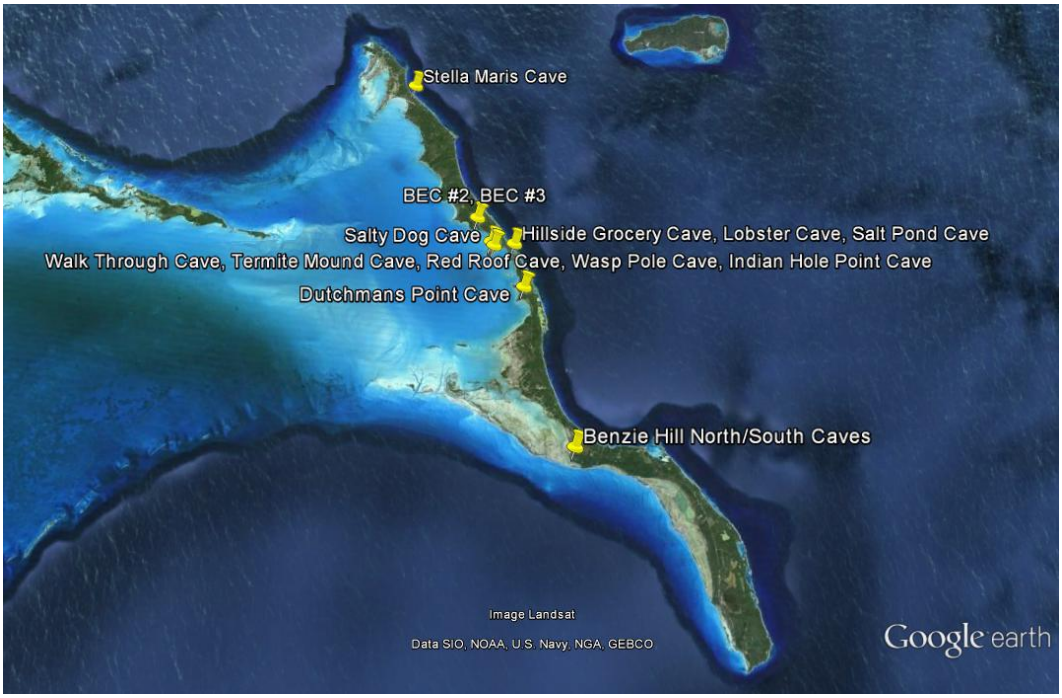

Figure 4.7 Caves used in the topographic map analysis plotted on Long Island (Google Earth, 2014).

Figure 4.8 Caves used in the topographic map analysis plotted on New Providence (Google Earth, 2014)

Figure 4.9 Caves used in the topographic map analysis plotted on San Salvador (Google Earth, 2014)

A summary of those results is as follows: There were a total of 408 cave entrances. Of the 408 total, there were 123 side breach entrances, 185 pit entrances, and 100 collapse entrances recorded. Signs of roof collapse were absent in 61 of the 107 caves analyzed. As previously stated, if the hole in the roof was small and no collapse breccia was noted on the floor of the cave, the entrance classification was assigned as a pit intersection. Histograms of slope vs entrance type are shown in Figures 4.10, 4.11, 4.12, 4.13. Rare slopes greater than 14 degrees are not included (all having side entrances). These slopes range from 17 to 45 degrees, accounting for 12 slopes and 15 side entrances. The four caves with 45-degree slopes are actually short caves in bedrock towers with vertical walls and flat tops. The calculation of rise over run in these cases creates a 45-degree slope value, where the slope starts as a 90-degree wall and ends as a zero degree flat top. The full data are in Appendix A. The histograms of slope vs entrance type (total, side, collapse, and pit) do not indicate a relationship detectable between slope and any single type of entrance type (Fig 4.14) from topographic data of 20 ft (6 m) resolution.

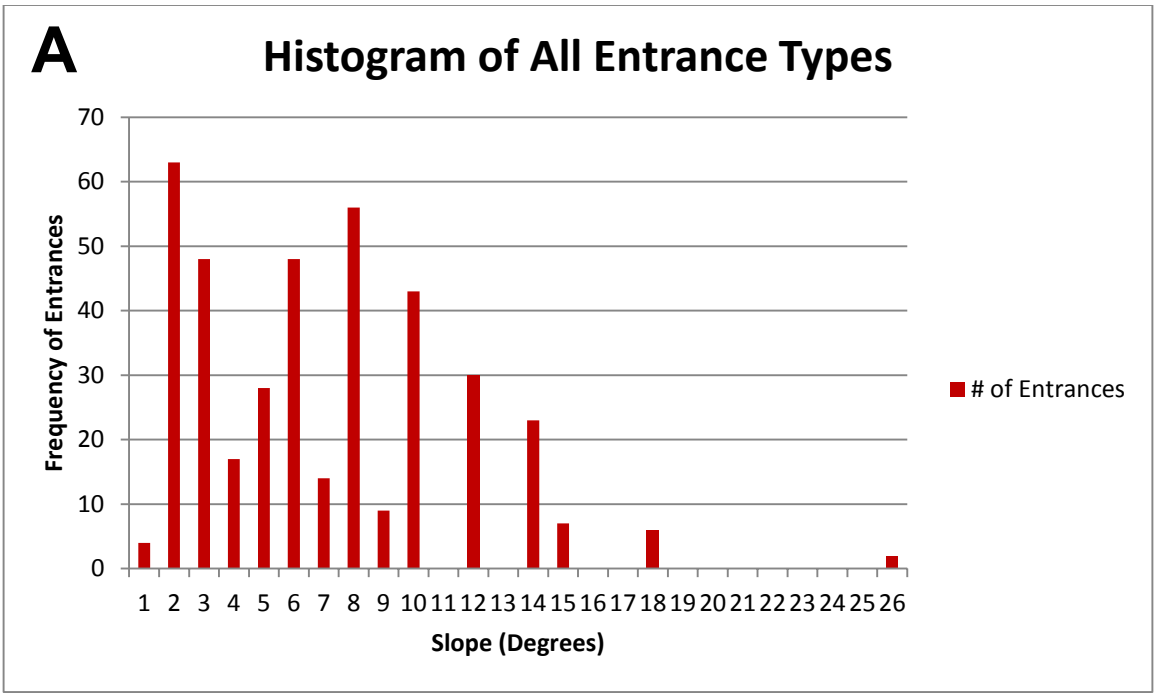

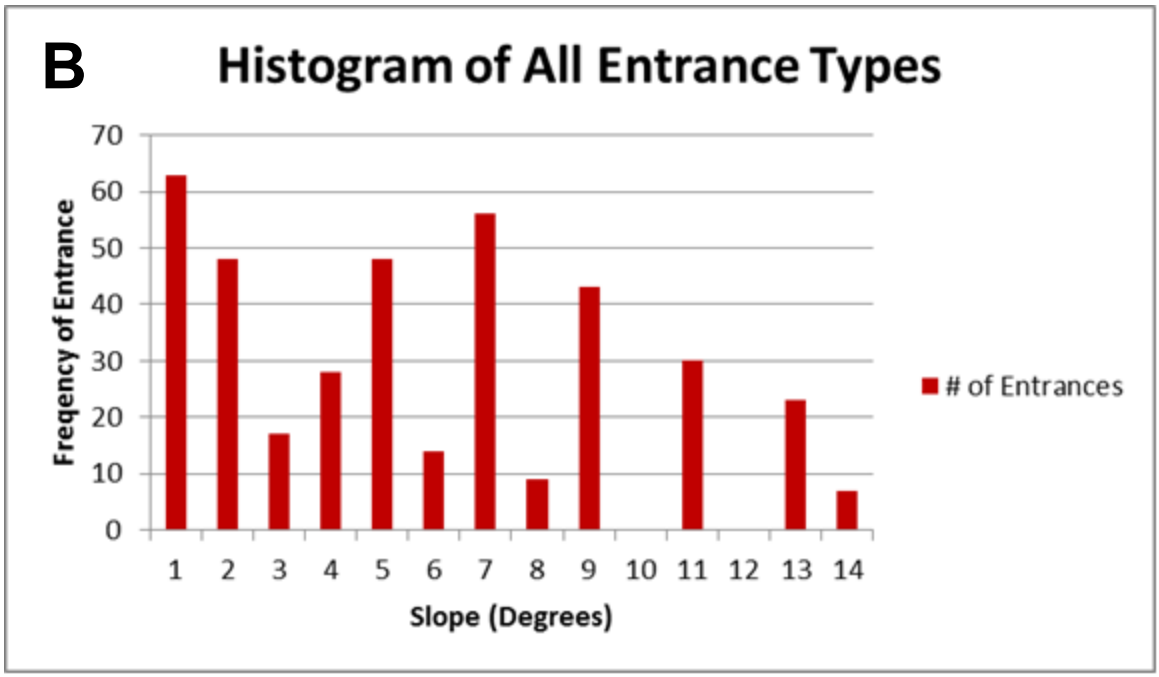

Figure 4.10 A) Histogram of slope vs the number of total entrances for each of the 103 caves in the topographic map study. B) Histogram of slope vs the number of total entrances for 95 of the caves in the topographic map analysis. For Figures 4.10B to 4.17, slope values above 14 degrees not displayed; see text for explanation.

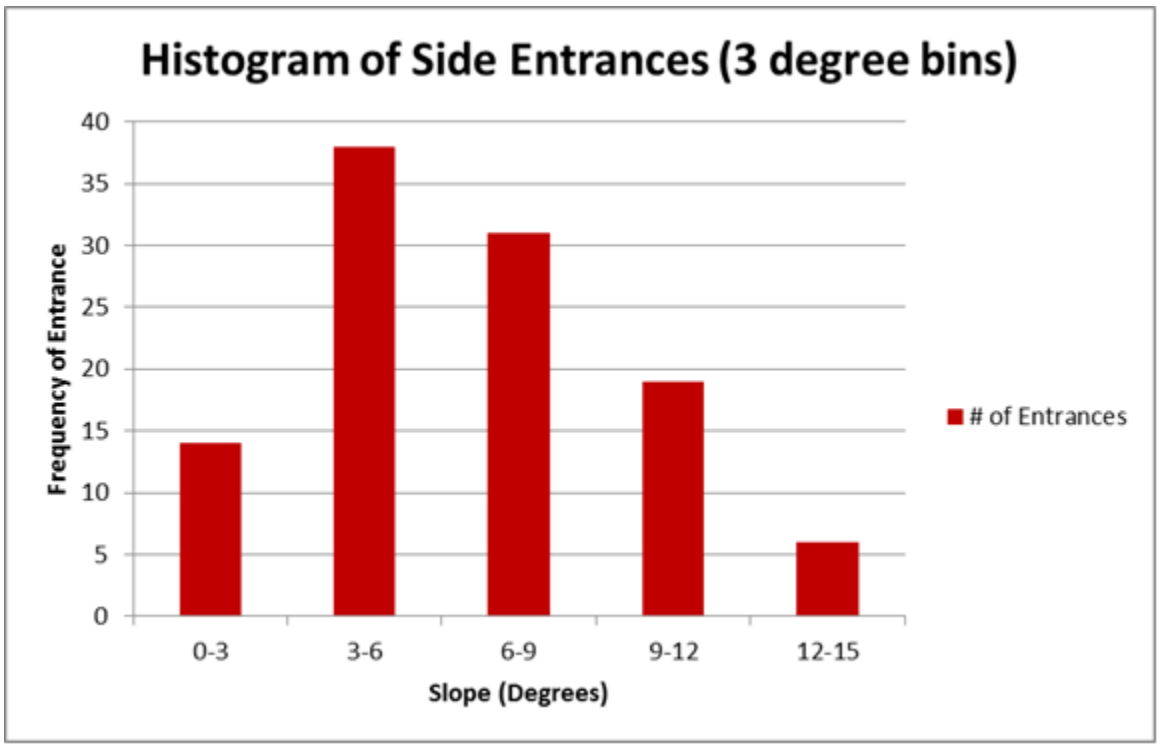

Figure 4.11 Histogram of slope vs the number of side breach entrances for each of the 95 caves in the topographic map analysis.

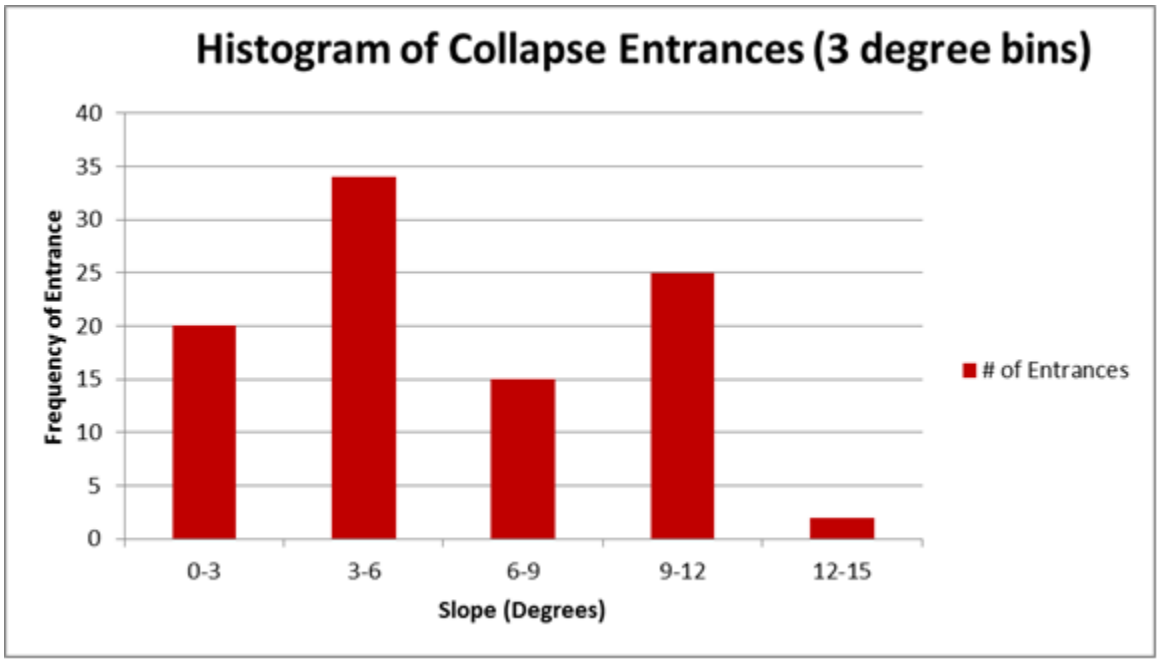

Figure 4.12 Histogram of slope vs the number of collapse entrances for each of the 95 caves in the topographic map analysis.

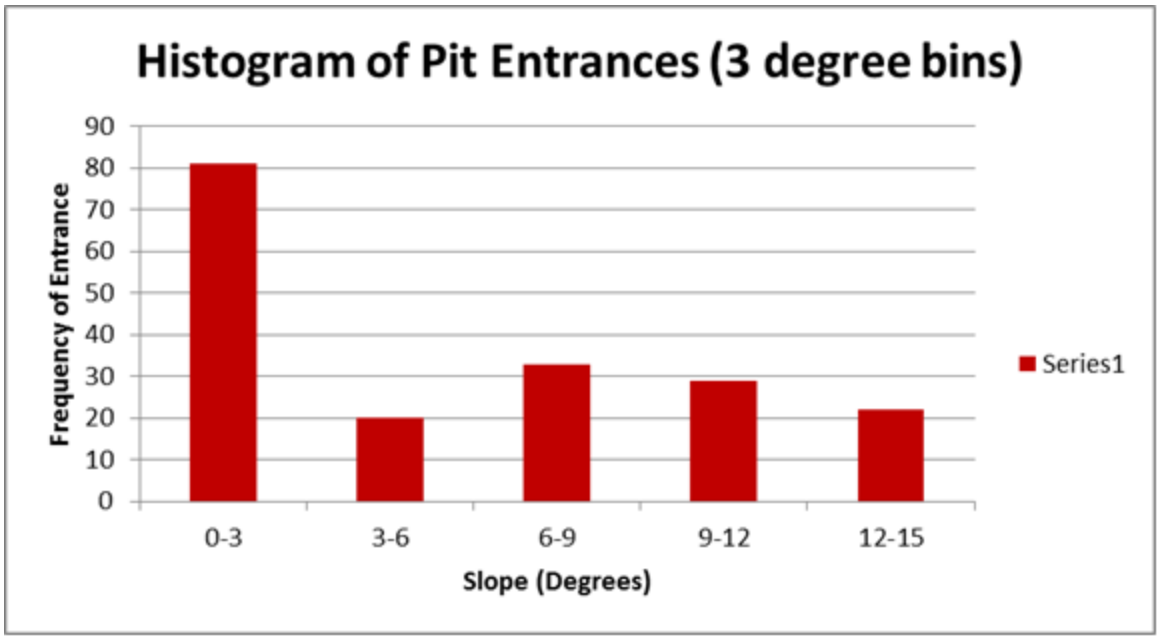

Figure 4.13 Plot of slope vs the number of pit entrances for each of the 95 caves in the topographic map analysis.

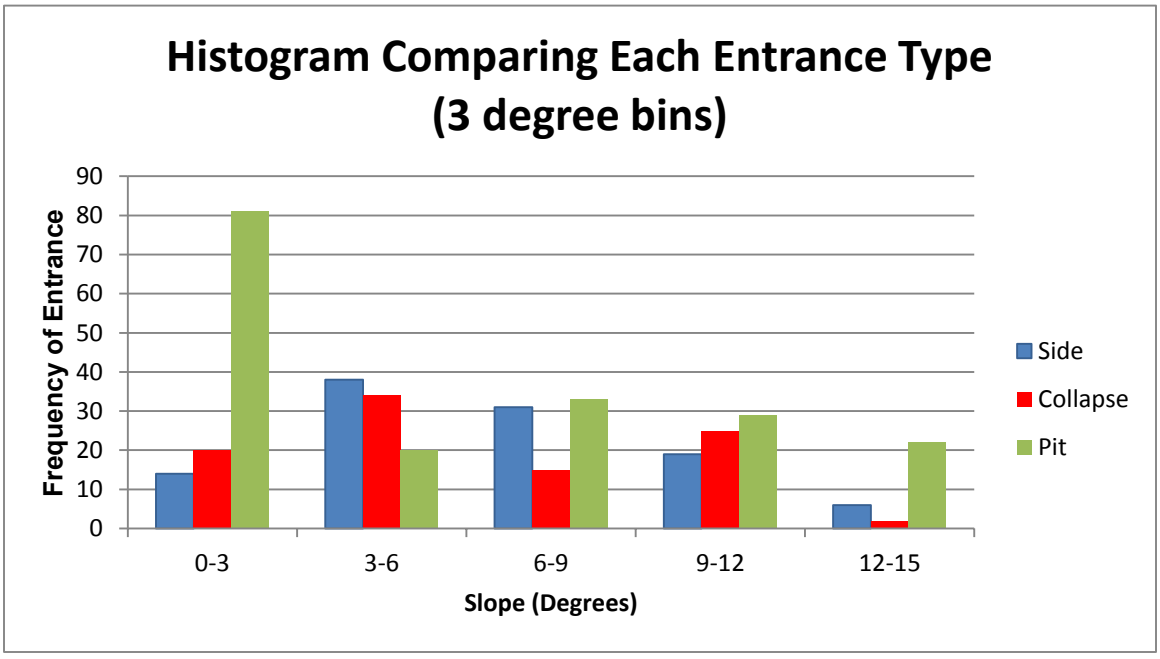

Figure 4.14 Histogram of each entrance type for 95 caves using a three degree bin size. Note that the entrance types occur across all slopes from gentle to steep.

Each cave in the study had one slope measurement. The total number of slope measurements of each unit slope value was plotted to determine the slope abundance for each slope (14 degrees or below) used in the study (Fig 4.15). Both side and collapse breaches are a result of large scale surface erosion (mechanical processes), unlike pit entrances which form by dissolution (chemical processes). For this reason the number of surface erosion cave entrances (side and collapse) per cave were plotted along with slope abundance (Fig 4.16); the number of cave entrances exceeds slope abundance. Therefore, most caves have more than one macroscopic entrance, expected as 408 entrances were recorded for 107 caves. Combining side and collapse entrances produces an entrance-to-cave ratio of 223/107 = 2.08. Figure 4.16 shows that the approximate ratio of 2 side-plus-collapse entrances per cave is also observed as approximately 2 side-plus-collapse entrances per slope segment. The distribution of pit entrances differed from that of side and collapse entrances (Fig. 4.17). The ratios of entrance type abundance per slope abundance is shown in Table 4.1.

Table 4.1 The ratio of entrance type abundance per slope abundance

Slope	Ratio of Total Entrances to Slope Abundance	Ratio of Side Entrance to Slope Abundance	Ratio of Collapse Entrance to Slope Abundance	Ratio of Pit Entrance to Slope Abundance	Ratio of Surface Erosion Entrances to Slope Abundance
0	4.00	0.00	2.00	2.00	2.00
1	15.75	1.00	1.00	13.75	2.00
2	4.80	1.00	1.40	2.40	2.40
3	2.83	0.83	1.00	1.00	1.83
4	2.33	1.33	0.50	0.42	1.83
5	3.00	1.06	1.38	0.56	2.44
6	1.75	0.88	0.75	0.13	1.63
7	5.60	1.70	0.70	3.20	2.40
8	2.25	1.75	0.50	0.00	2.25
9	5.38	0.88	2.00	2.50	2.88
10	0.00	0.00	0.00	0.00	0.00
11	2.73	1.09	0.82	0.82	1.91
12	0.00	0.00	0.00	0.00	0.00
13	11.50	1.00	0.00	10.50	1.00
14	2.33	1.33	0.67	0.33	2.00

The number of each cave entrance type is divided by each slope values' number of occurrences in the study.

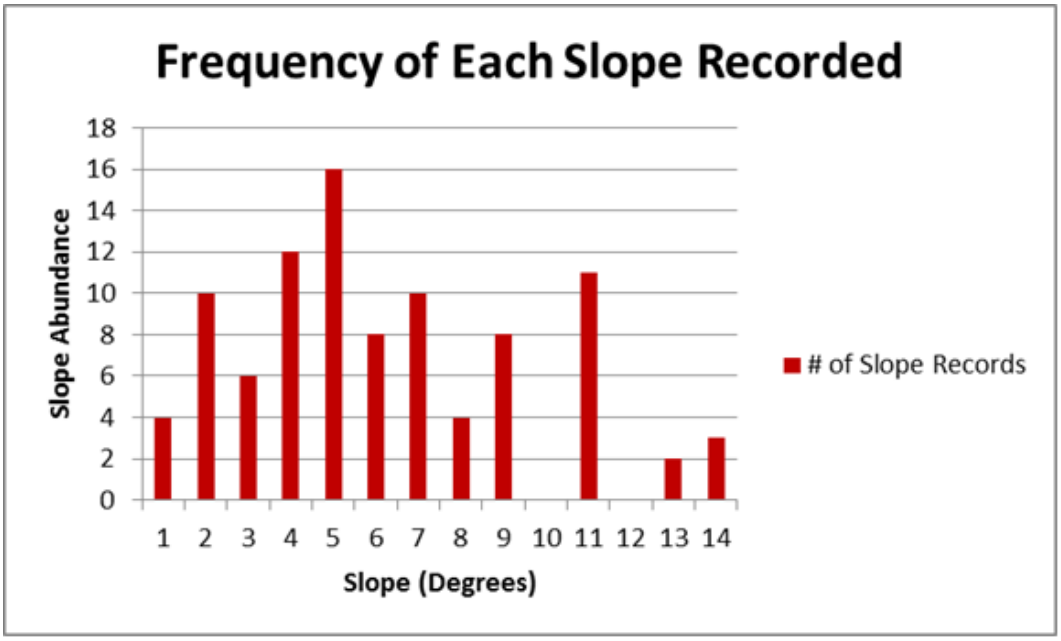

Figure 4.15 Shows the frequency of each slope measurement for 95 caves used in the study.

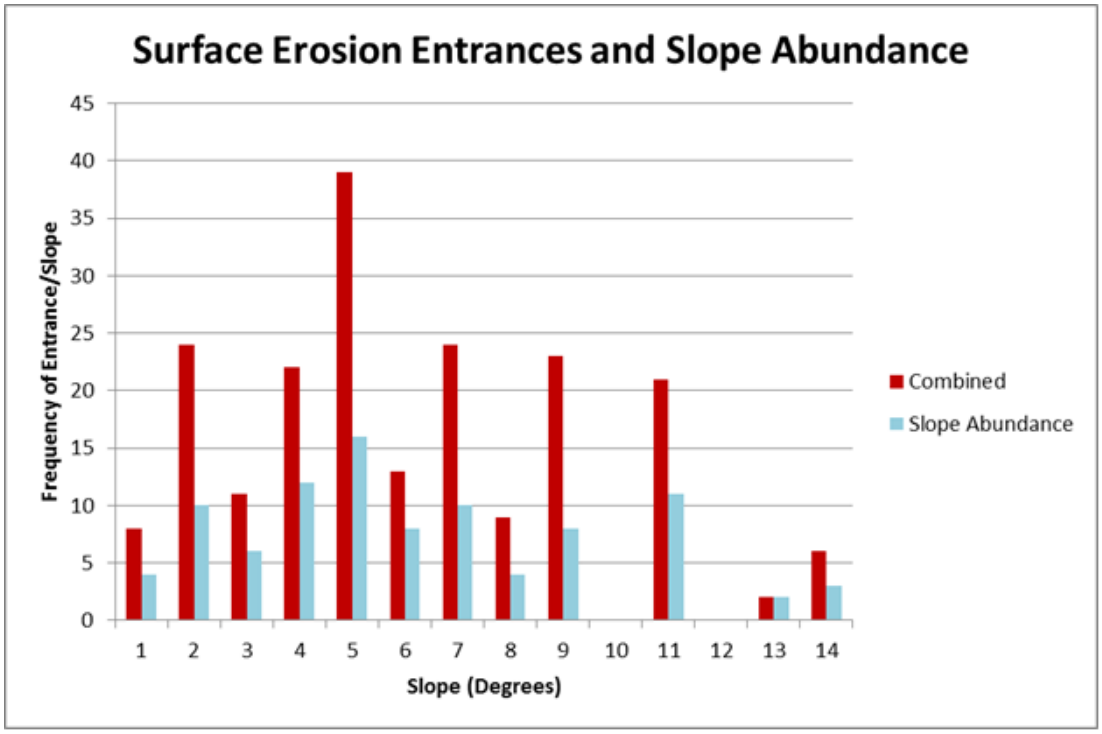

Figure 4.16 Side and collapse breaches combined comparing to the abundance of each slope.

Note that the number of entrances per slope value is approxamately 2 times the slope abundance.

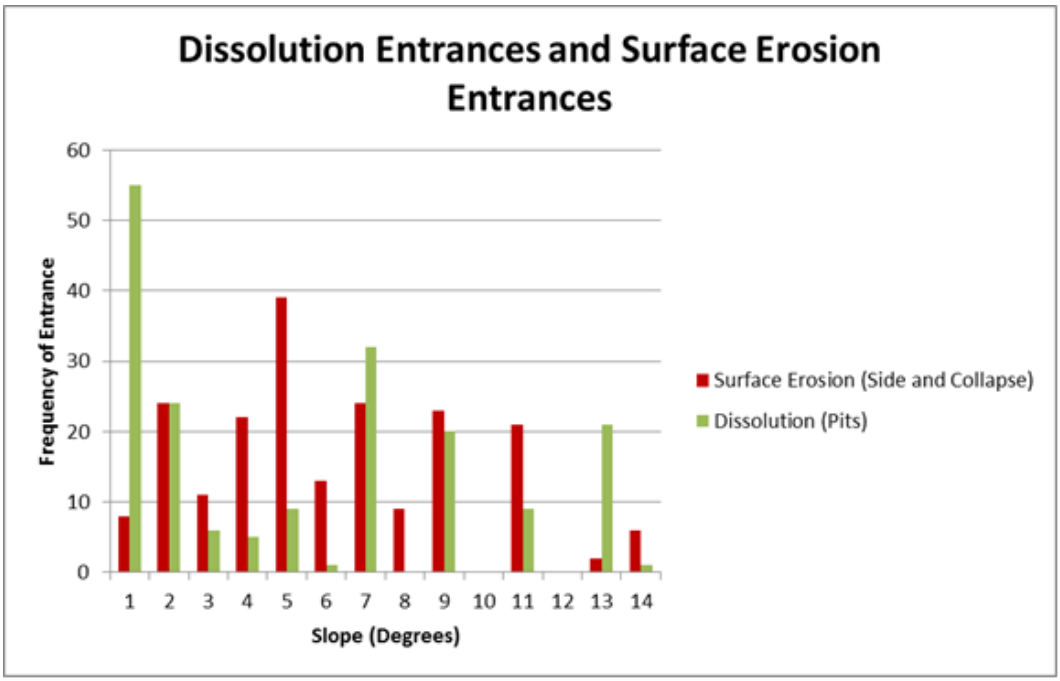

Figure 4.17 Shows the distribution of pit entrances differing from that of the combined surface erosion entrance types (side and collapse).

Chamber size (maximum chamber width) was analyzed to see what effect it may play in collapse risk. The slope for each cave, along with the chamber size was plotted on a histogram for each of the caves in the study (Fig 4.18). This plot allows the variance in chamber size to be observed, and helps the user realize how unpredictable chamber size is. Since chamber size and roof thickness are coupled as the causes for collapse, this unpredictability of chamber size further complicates using slope as a predictor of collapse.

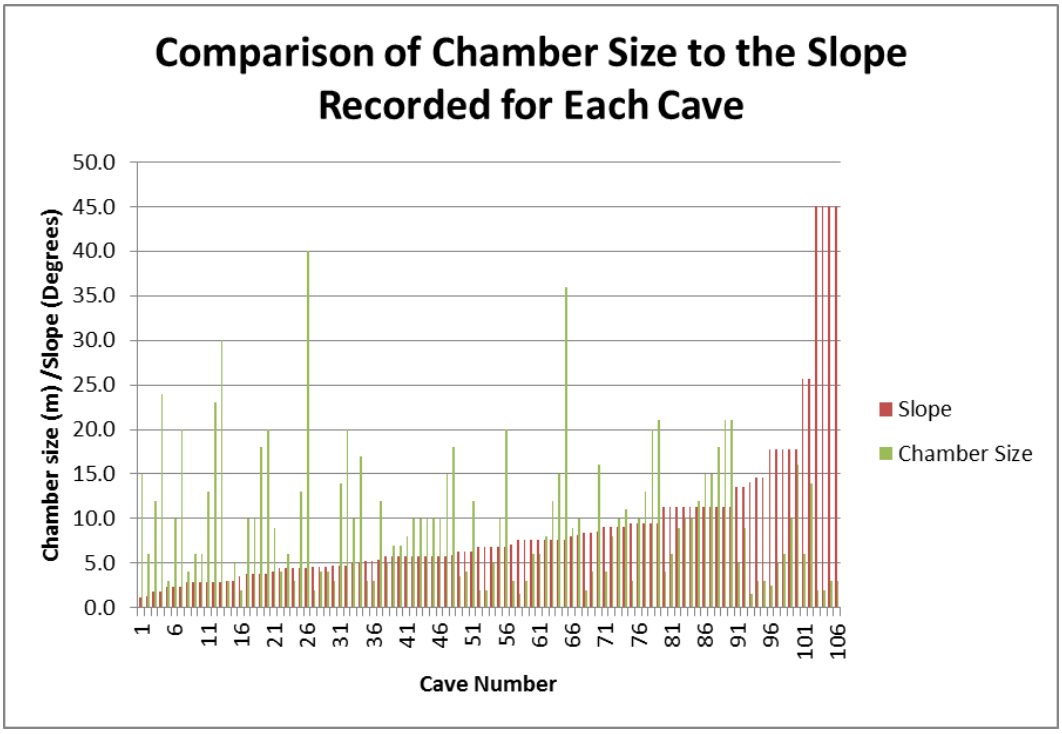

Figure 4.18 These data exemplify that the size of the void at depth varies greatly independent of the slope (e.g., the same size void is plotted at 3, 6, 9, and 12 degrees). Therefore, collapse cannot be predicted using slope by itslef, as the chamber size effects the roof support.

Following the topographic map analysis, a smaller case study used six caves that have been field surveyed (1 m contours). The same methods used for the topographic map analyses were used on these six surveys. These data do not suggest that there is a strong relationship (Fig 4.19) between slope and entrance type. The real relationship would be slope to roof thickness, as roof thickness (a proxy for beam thickness) coupled with chamber width is what allows the collapse to occur. The six-cave case study provides data shown in Table 4.2.

Table 4.2 Shows the variation in the hillslope using the higher resolution field surveyed data to calculate slope.

Cave Name	Transect	Hillslope
1702 Cave	a	8.3
	b	21.8
	c	4.9
	d	3.4
Hatchet Bay Cave	a	7.8
	b	5.5
	c	5.7
	d	4.8
Ten Bay Cave	a	2.7
	b	2.5
	c	5.7
	d	6.0
Maroon Hill Cave	a	9.0
	b	3.4
	c	11.3
Salt Pond Hill Cave	a	6.1
	b	2.0
	c	2.9
Lighthouse Cave	a	18.4

Transects for each cave can be located in Fig 4.26, 4.27, 4.28, 4.29, 4.30, 4.31.

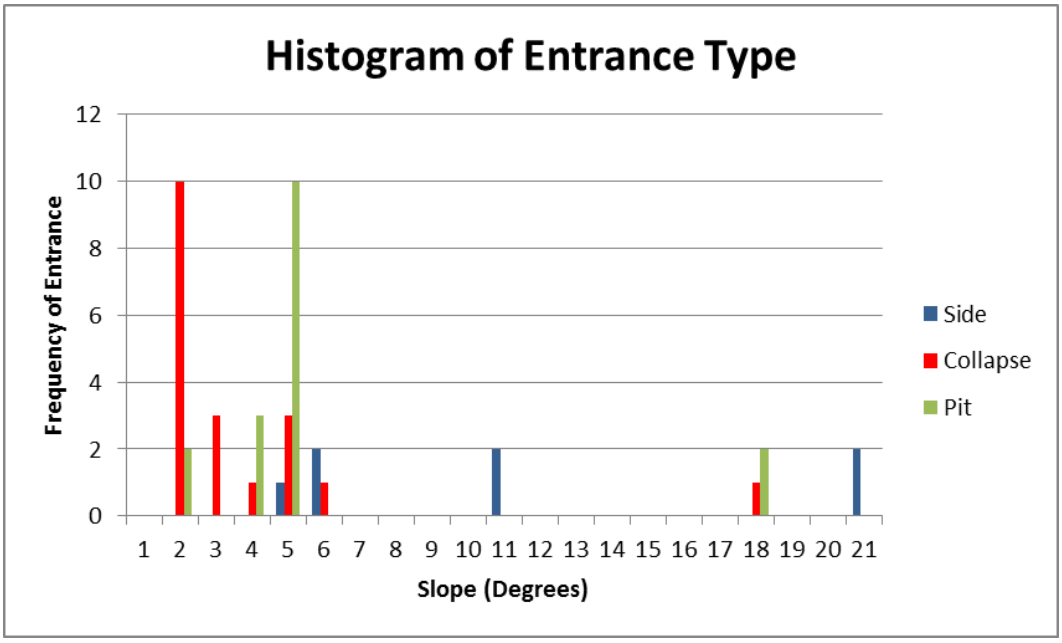

Figure 4.19 Histogram of entrance type vs slope for the six caves used in the 1 m field surveyed map analysis.

The slope was calculated over each section of collapse.

These data were extracted from cave maps with the field surveyed (1 meter) contours overlaid (Fig. 4.20, 4.21, 4.22, 4.23, 4.24, 4.25). The higher resolution of spatial data leads to a more detailed analysis; these data allowed the slope to be calculated over the entire cave as well as the slope over the sections that showed collapse (Fig. 4.26, 4.27, 4.28, 4.29, 4.30, 4.31). A visual comparison of the two data types helps to clarify the limitations of this study (Fig. 4.20, 4.21, 4.22, 4.23, 4.24, 4.25). Figure 4.19 does show some trends. Side entrances fall towards the high slope angle end of the plot, collapse entrances towards the low slope angle end of the plot. Pit caves are strongly biased to the lower slope angles.

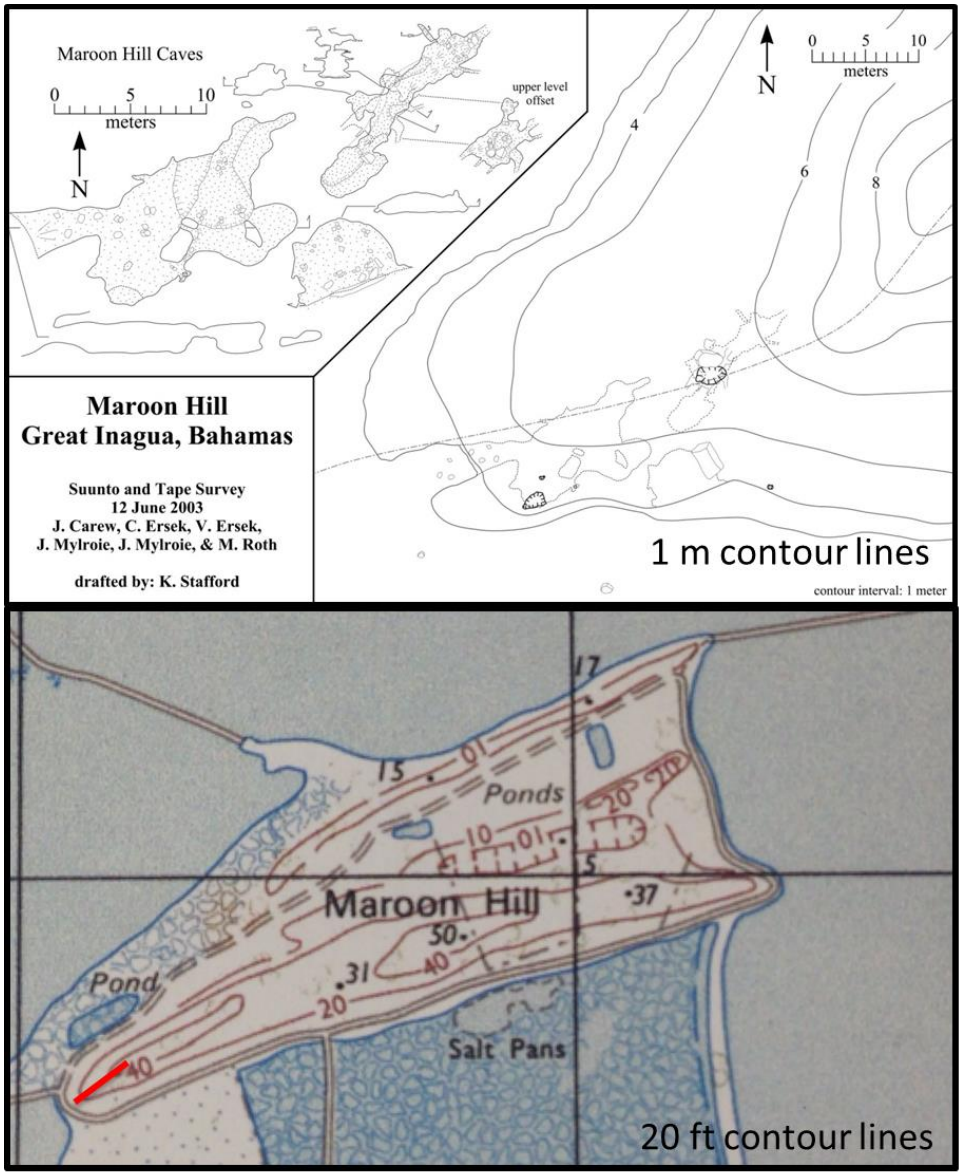

Figure 4.20 Shows the resolution difference between the topographic map (20 ft contours; bottom) and the field surveyed map (1 m (3 ft) contours; top) to provide a understanding of the limitations of the study.

Notice the collapse is in areas where the contours are more spread out, indicating a more gentle slope.

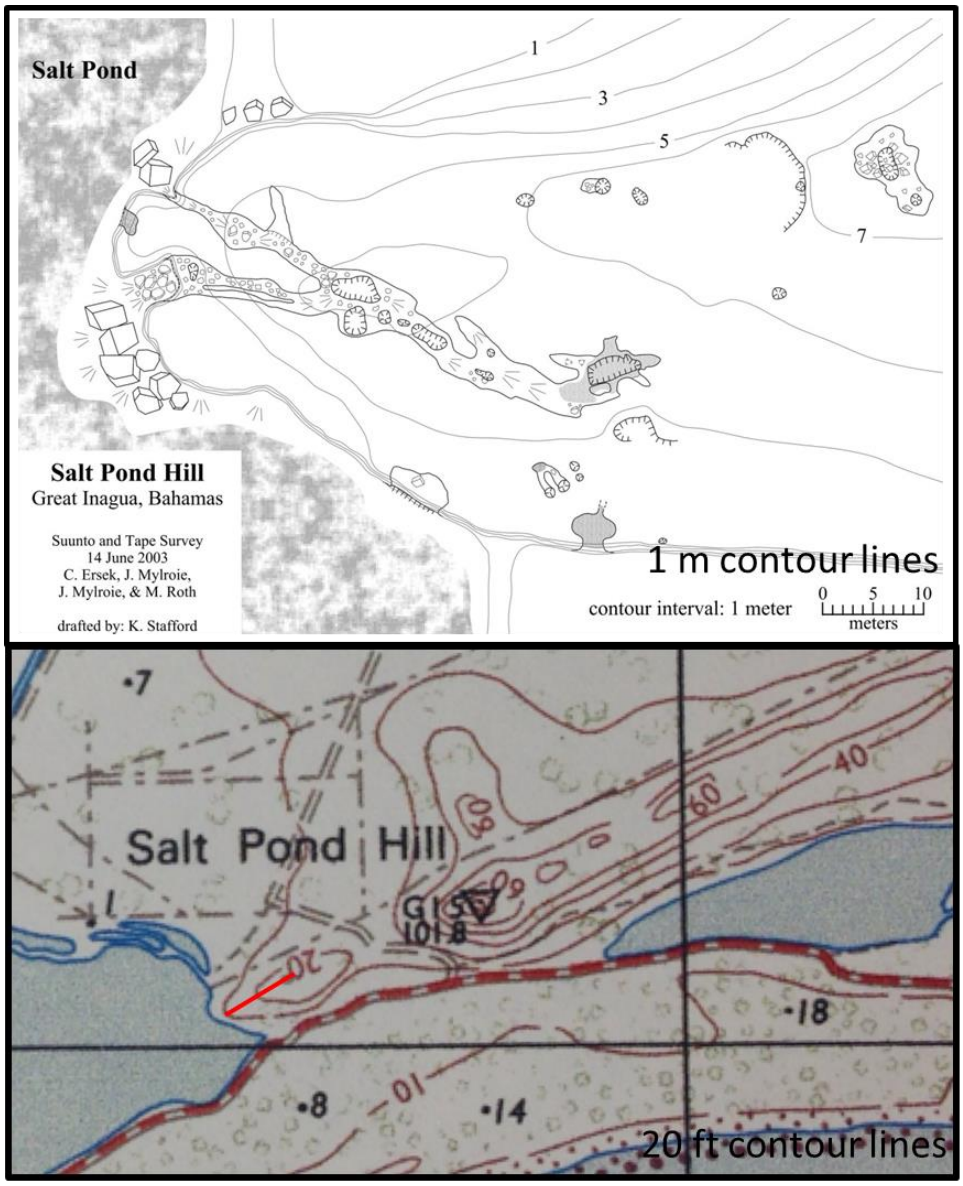

Figure 4.21 Shows the resolution difference between the topographic map (20 ft contours; bottom) and the field surveyed map (1 m (3 ft) contours; top) to provide a understanding of the limitations of the study.

Notice the collapse is in areas where the contours are more spread out, indicating a more gentle slope.

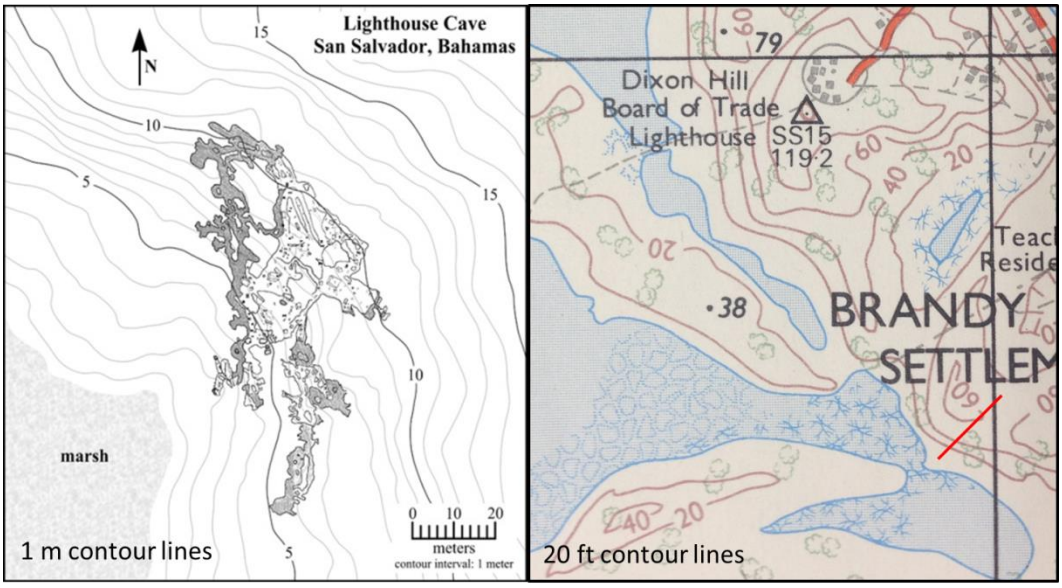

Figure 4.22 Shows the resolution difference between the field surveyed map (1 m (3 ft) contours; left) and the topographic map (20 ft contours; right) and to provide an understanding of the limitations of the study.

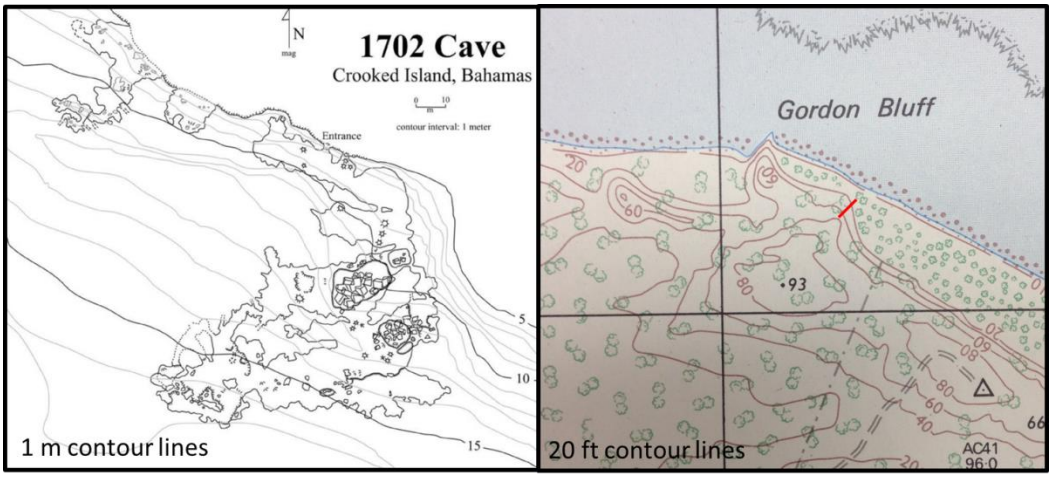

Figure 4.23 Shows the resolution difference between the field surveyed map (1 m (3 ft) contours; left) and the topographic map (20 ft contours; right) and to provide an understanding of the limitations of the study.

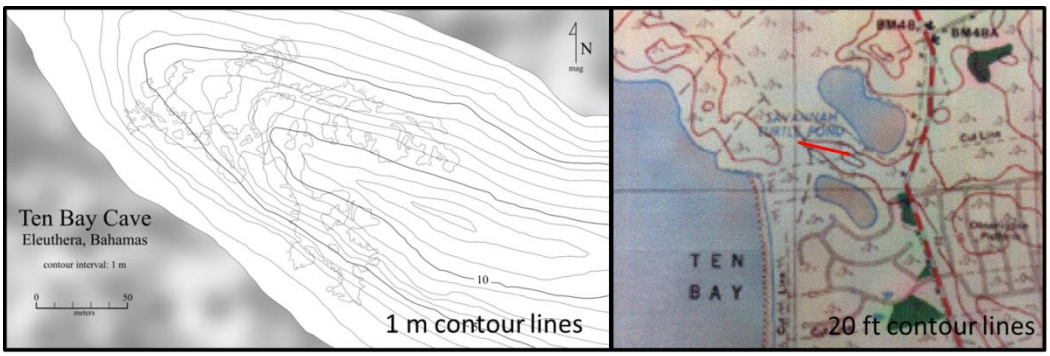

Figure 4.24 Shows the resolution difference between the field surveyed map (1 m (3 ft) contours; left) and the topographic map (20 ft contours; right) and to provide an understanding of the limitations of the study.

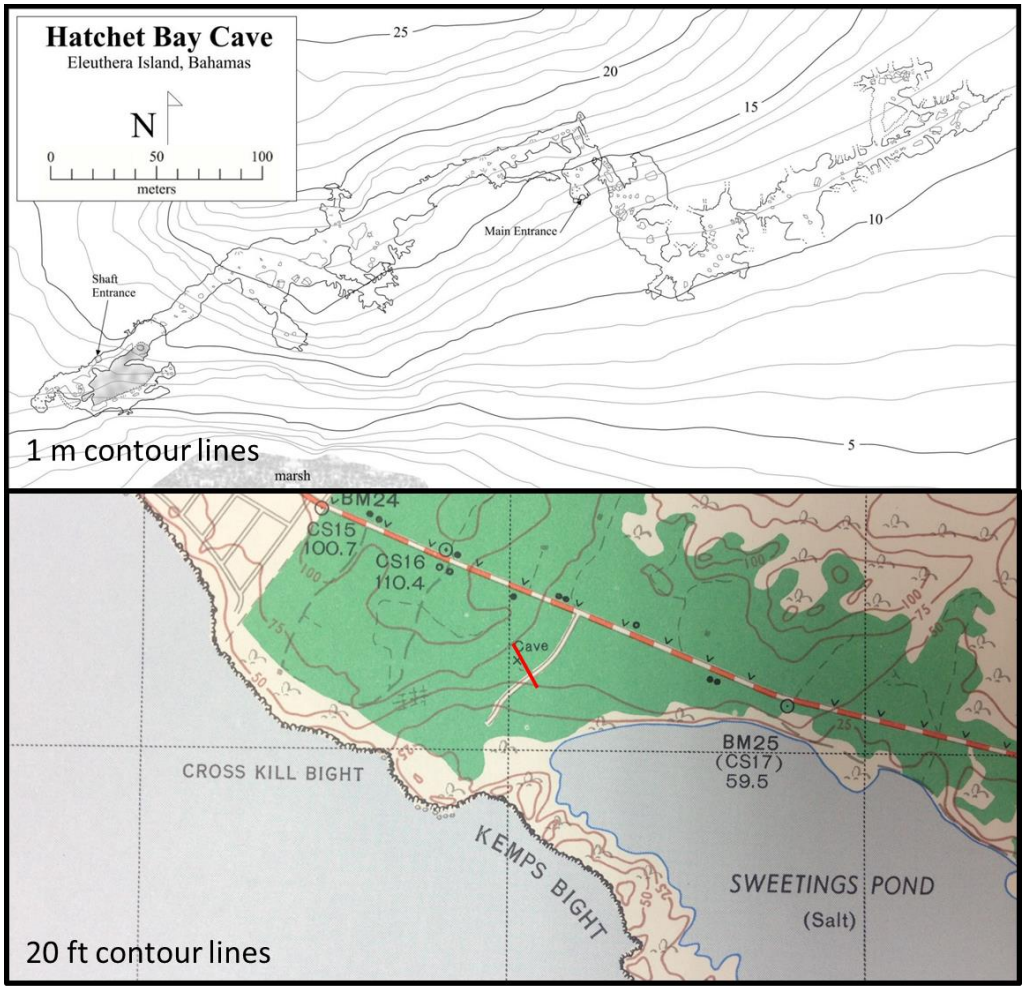

Figure 4.25 Shows the resolution difference between the topographic map (20 ft contours; bottom) and the field surveyed map (1 m (3 ft) contours; top) to provide a understanding of the limitations of the study.

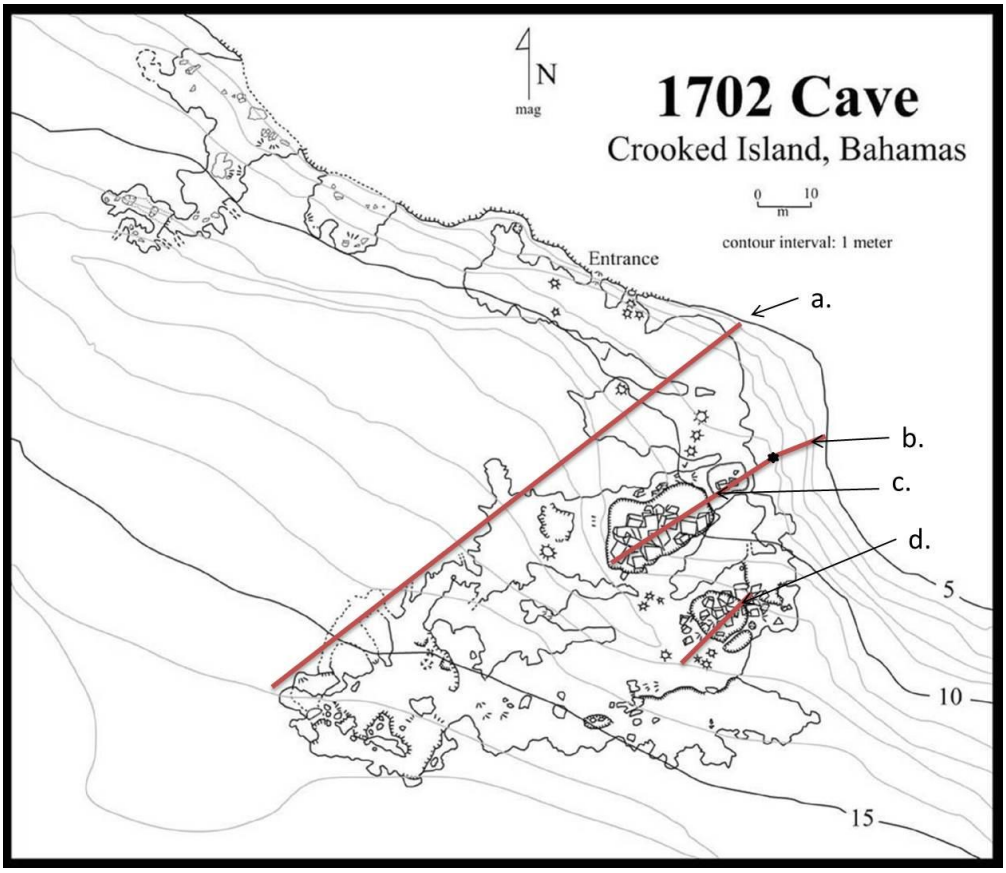

Figure 4.26 Shows the transects drawn in to illustrate where the slope was calculated. The transect letters correspond with Table 4.3. Note the slope over areas with collapse (c and d).

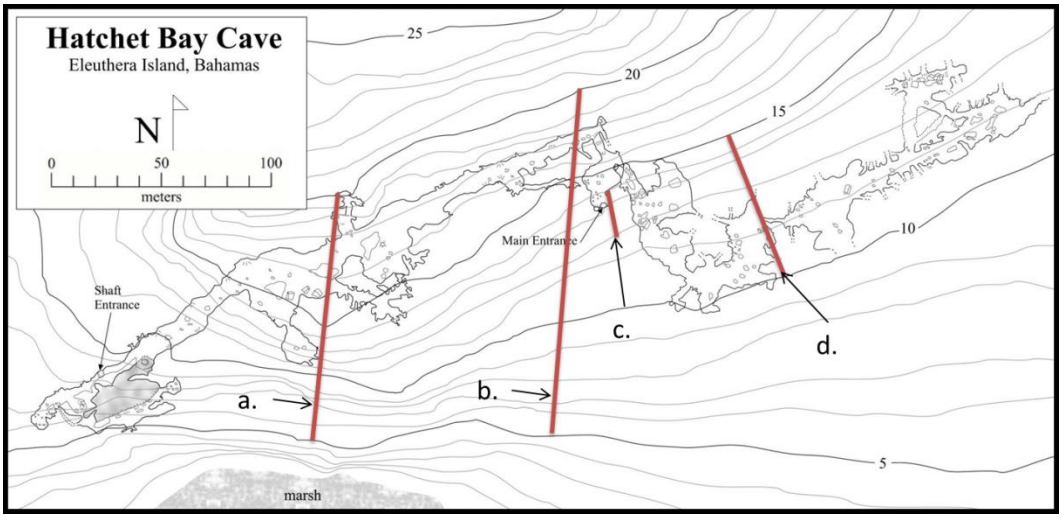

Figure 4.27 Shows the transects drawn in to illustrate where the slope was calculated. The transect letters correspond with Table 4.3.

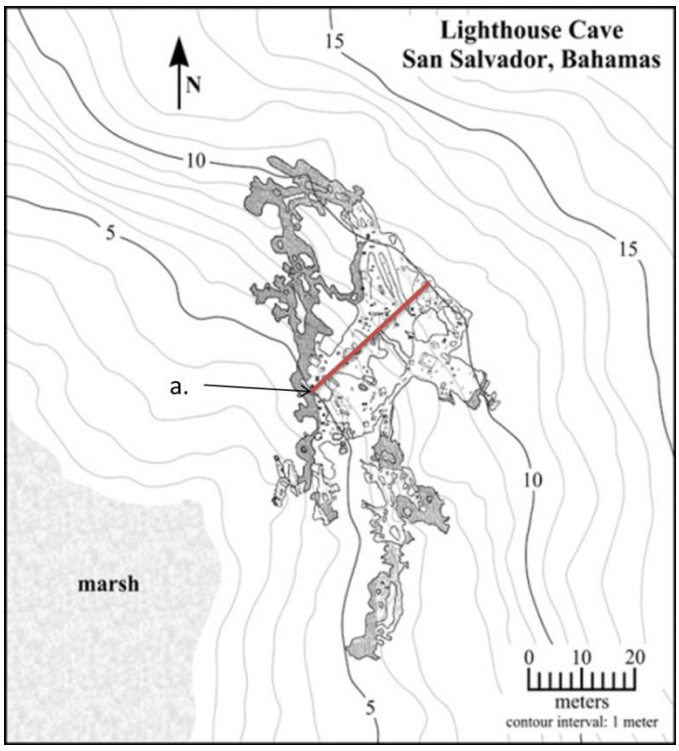

Figure 4.28 Shows the transects drawn in to illustrate where the slope was calculated. The transect letters correspond with Table 4.3.

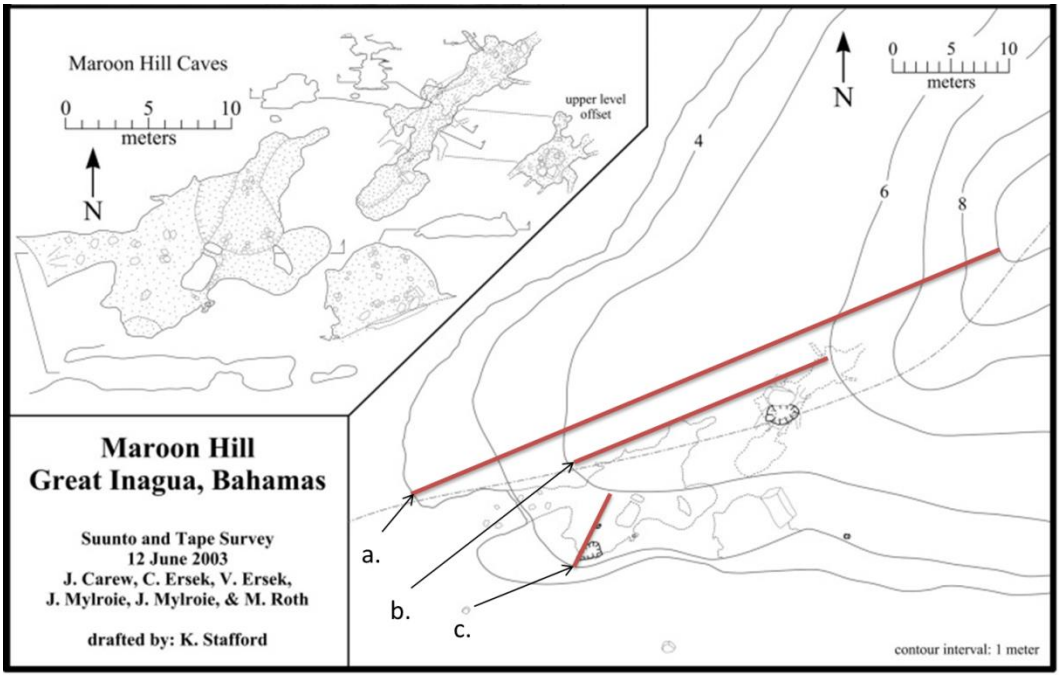

Figure 4.29 Shows the transects drawn in to illustrate where the slope was calculated. The transect letters correspond with Table 4.3.

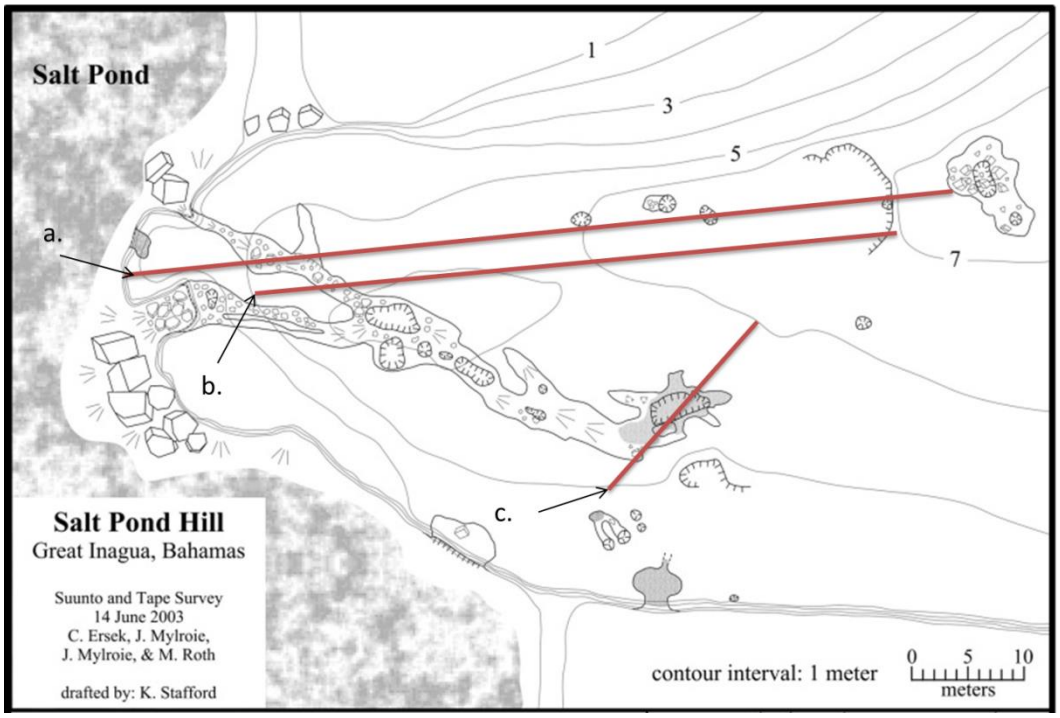

Figure 4.30 Shows the transects drawn in to illustrate where the slope was calculated. The transect letters correspond with Table 4.3.

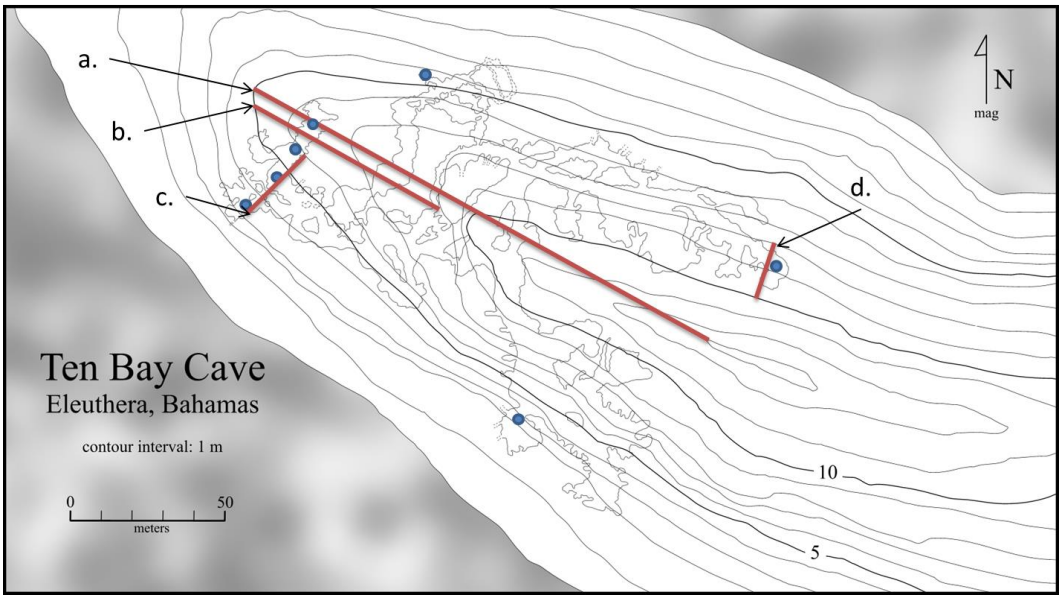

Figure 4.31 Shows the transects drawn in to illustrate where the slope was calculated. The transect letters correspond with Table 4.3.

At this point, a realization was made that the accuracy of the calculated slope was not good enough to estimate roof thickness from the cave map data. The original methodology included a few steps that incorporated the estimation of roof thickness for areas of collapse using the calculated slope from the topographic maps, but due to the limitations of the data accuracy, these methods were not performed.

CHAPTER V

DISCUSSION

Topographic Map Analysis

This project focused on whether or not 7.5-minute topographic map sheets could be used to predict cave roof collapse; the resolution of the topographic maps does not allow such predictions to be produced. Using the calculated slope of 107 caves from data extracted from the topographic map sheets is based on the idea that slope can be used as a proxy for roof thickness (roof thickness being one of the critical components that initiates collapse). The resolution of the currently available topographic data allows the roof overhead to be crudely estimated using the slope derived from the topographic maps, but this slope is not accurate enough to determine roof thickness as the spatial data limitations are simply transferred. The variations in the hillslope, which are not noticeable from the topographic maps, can lead to an inaccurate roof thickness reading. With many areas having terraced slopes (Fig 5.1, 5.2), the roof thickness can vary much over what appears to be a steady slope on the topographic maps but is not so in the real world. The map of 1702 Cave (Fig 4.26) is an excellent example of how the flat areas (wider contour spacing) allows for collapse. If the elevation for both examples from Fig 5.1 (A) and (B) were extracted from topographic maps with 20 ft (6 m) contour lines and was used to calculate the slope, approximately the same slope would be derived for these two obviously different dune profiles. When the elevation data for both examples from

Fig 5.2 (A) and (B) were extracted from the field surveyed 1 m contour maps and was used to calculate the slope, the slopes for (A) and (B) would be much different. The problem with this approach is that with the resolution of topographic map sheets, if a prediction model was made, it would be misleading (much like the example using Figure 5.1). In turn, the model could overlook a collapse risk (e.g. say that it is safe to build) by assuming a steady slope when in reality the landscape may have a varying slope (introducing flat areas with potentially thin roofs). If this model was constructed using inadequate spatial resolution, it could result in someone building in a location that is actually prone to collapse (on accident). The worst-case scenario of this development would be a collapse event resulting in loss of life, time, and/or investment capital.

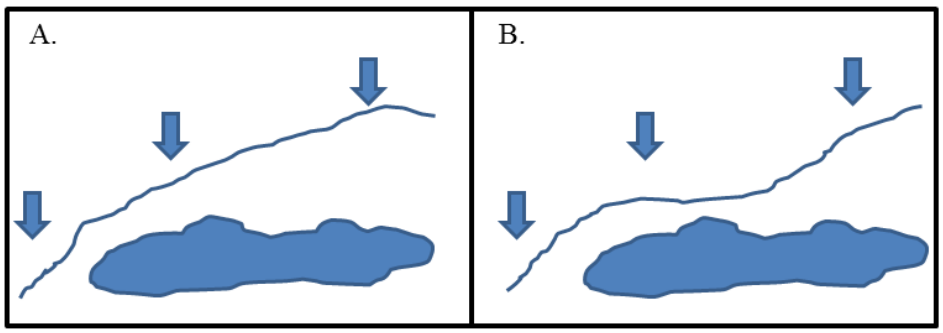

Figure 5.1 Topographic profiles of two dunes overlying an identical void at depth.

Using 6 m contour lines to calculate slope for these two profiles, the two slopes would appear to have approximately the same slope. A. Example of a dune with steady slope. B. Example of a dune with a variation in hillsope. Note that collapse would be expected in B, but collapse would not predicted if using the slope calculated from the data collection points shown above (arrows).

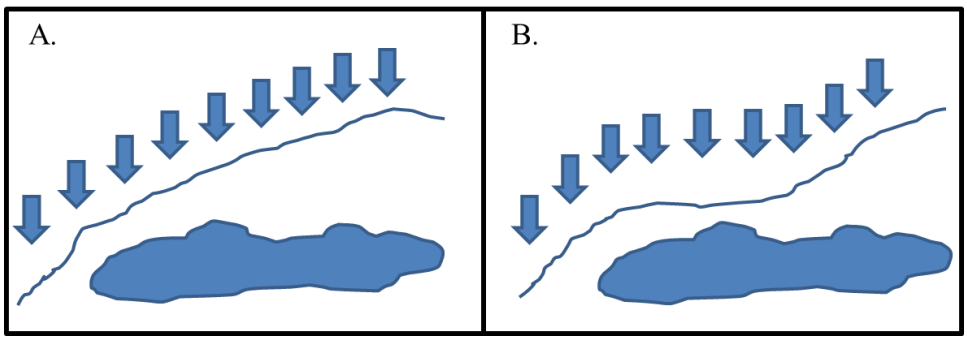

Figure 5.2 Topographic profiles of two dunes overlying an identical void at depth.

Using 1 m contour lines to calculate slope for these two profiles, the two slopes would differ greatly and allow for much more accurate prediction. A. Example of a dune with a steady slope. B. Example of a dune with a variation in hillslope. Note that collapse would be expected in B, and that the collapse could be predicted when using the higher resolution (1 m) elevation data.

Flank margin cave entrances are interesting due to the fact that flank margin caves form as entranceless voids beneath the surface (Fig 1.1). The caves remain entranceless until the cave is breached by cliff retreat (side entrance), roof collapse (overhead entrance due to roof thickness and unsupported span), or pit intersection (overhead entrance occurs by localized active dissolution). The 408 cave entrances consisted mostly of pit entrances (185); pits are typically the smallest type of entrance. Side breach entrances were the next most common entrance type (123) and are the largest entrance type, typically allowing one to walk/crawl into the cave from the side. Collapse breaches (100) are the most dangerous entrance type and often have a large area of collapse over gentle slopes. Side breach entrances are common near the coastline or where cliff retreat has occurred, commonly a steeper slope (e.g. Figure 4.19; transect (c) in Fig 4.29). Pit entrances are non-selective to their location of formation; pit entrances occur by the downward dissolution of rock as explained by epigenic karst processes (meteoric water). Side breach

and collapse entrances are the result of processes that occurred after the hypogenic speleogenesis of the cave was complete; pit entrances form by active epigenic speleogenesis. Many caves with the same overlying slope had a different entrance type, supporting the notion that is more than just roof thickness that effect collapse; chamber width coupled with roof thickness controls the initiation of collapse. Chamber size and the slope for each cave were plotted together in a histogram, and as expected, there is no relationship between these two variables. Flank margin caves are de-coupled from surface processes, and their formation is controlled by the geochemistry and flow dynamics of the fresh-water lens margin. Therefore, as Figure 4.18 demonstrates, chamber size has no relationship to slope.

On the data plots for the 7.5 minute topographic maps, pit entrances show a relationship with low angle or gentle slopes (Figure 4.13). That relationship persists when the slope is calculated from a 1 m contour survey (Figure 4.19). Side and collapse entrances seem to show a relationship to gentle to moderate slopes (Figures 4.11 and 4.12), but that apparent relationship is an artifact of slope abundance, as Figure 4.16 demonstrates when side and collapse entrances are combined as a single mass wasting entrance type, the ratio of those entrances to slope abundance stays around 2 (Table 4.1). When the more detailed slope analysis using 1 m contours is displayed (Figure 4.19), collapse and pit entrances clustered near the low slope end of the plot and side entrances at the middle or high end of the plot.

The distribution of entrances as to slope angle is based on entrance origin. Pit entrances result from localized vadose flow dissolving its way downward. These pits are commonly only a few meters deep, but they can be as much as 10 m deep on rare

occasions. When the slope is low, the amount of rock over the cave is less than when the slope is steep (Figures 5.1 and 5.2). As a result, a dissolution pit only a few meters deep is more likely to enter a cave when the slope is low and the roof is thin, regardless of the chamber size below and the amount of unsupported room span (Figure 5.3). As Figure 4.13 shows, pits can have a variety of depths, but small depths are more common, so while pit entrances are found on all slopes, they predominate at low slopes where the cave roof *must* be thin (under a steep slope, the cave roof can be thick or thin).

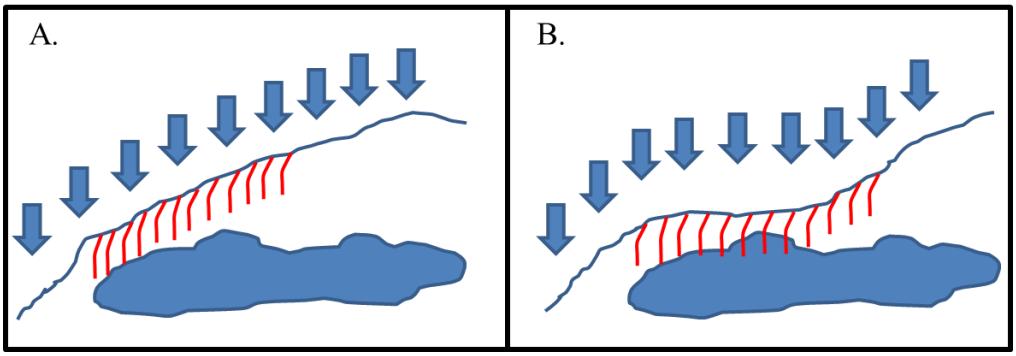

Figure 5.3 This figure shows two dunes with differing slopes overlying the same size void at depth.

The pit entrances drawn (red lines) depict how slope effects the occurrence of a pit entrance. Pit caves are shallow dissolution features, allowing them to intersect only the voids with thin roofs. A) The greater slope provides a thicker roof and prevents pit intersection from being common. B) The flatter, more gentle slope allows for pit intersection due to the thin roof conditions.

Collapse entrances result from roof failure, and the thinner the roof (low beam thickness), or the wider the chamber (high unsupported span value), or both, the more likely is roof collapse. However, chamber width has no relation to slope (Figure 4.18), so collapse can occur at any slope but does seem to occur mostly at lower slopes which would create a thinner bedrock roof (Figures 5.1 and 5.2). This slope preference is hinted

at in Figure 4.12, but is better displayed in Figure 4.19 when higher slope resolution is available.

Side entrances result from mass wasting and erosion of hillslopes. Because flank margin caves form under the flank of the land, at the distal margin of the fresh-water lens, to become exposed by surface erosion (as opposed to collapse or pit development) requires that the hillslopes retreat laterally so that the cave is intersected. The key is lateral retreat. The margin of a fresh-water lens during the last interglacial was at about 6 m elevation. A gentle slope starts out at an elevation below 6 m, and to reach that elevation must retreat significantly. A steep slope will reach the 6 m point after less slope retreat; a gentle slope must retreat farther to intersect a cave than a steep slope (Figure 5.4). While the data in Figure 4.11 are ambiguous regarding slope, the data in Figure 4.19 are much more convincing, with side entrances preferentially found at higher slope angles. Figure 4.19 again demonstrates the necessity of high resolution slope analysis.

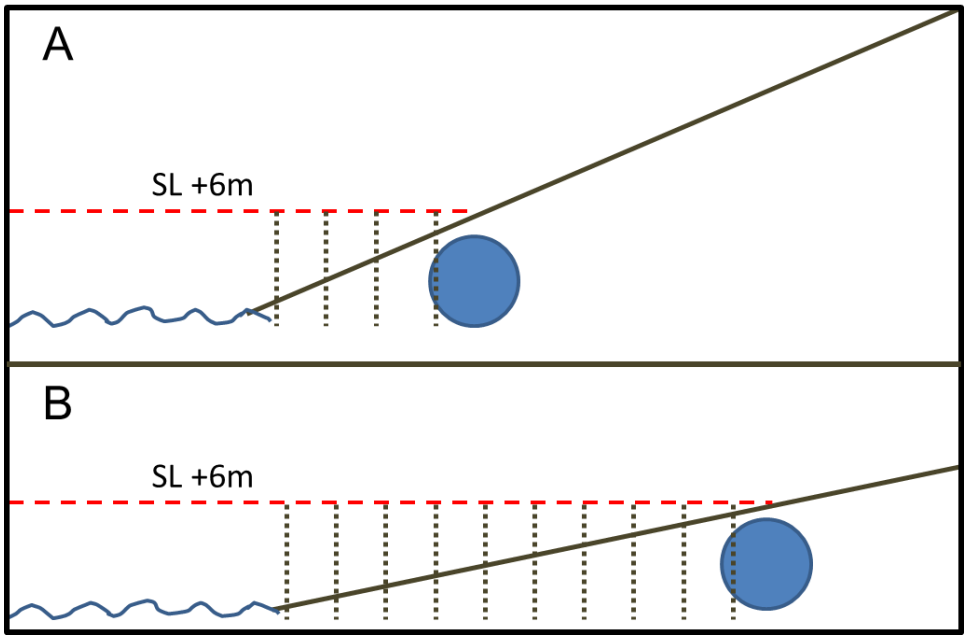

Figure 5.4 A) The steeper slope requires less cliff retreat to breach the cave by a side entrance. B) The more gentle slope requires more cliff retreat to breach the void.

Commonly, the steeper slopes result in side entrances, and the more gentle slopes result in roof collapse.

Unsupported Span

The beam thickness (a critical factor in predicting collapse) cannot be accurately assessed using the topographic maps produced by the Bahamas Lands and Surveys Department and therefore a prediction model cannot be constructed based on slope from that source. The combination of beam thickness (roof thickness) and unsupported span (maximum chamber width) explained by (White, 1988) controls roof collapse. Note that the unsupported span uses the maximum value for width – when a chamber size is measured, the longest measurement is typically the length and the lesser measurement is typically the width (i.e. the width is the shorter of the two measurements taken for chamber size). Several examples are presented next using cave (x):

Cave (x) - large span under a thin roof = may result in collapse

Cave (x) - small span under a thin roof = may not result in collapse

With a change in span or a change in roof thickness, at a certain threshold collapse would initiate. The proposed idea that slopes can be used as an indicator of roof thickness is based on the concept that:

Cave (x) – large span under a thick roof (steep slope) = may not result in collapse

Cave (x) – same span under a gentle slope (thinner roof) = may result in collapse.

The chamber size (maximum width) and slope was plotted for each cave to illustrate that chamber size and slope operate independently. The same void size is observable at a 3, 6, 9, and 12-degree slope. In addition, this plot helps to explain why some very gentle slopes do not demonstrate collapse; this could be because the void at depth has a small chamber size and the roof thickness is sufficient to support the roof span against the forces of gravity. For use as a prediction model in the future, it is important to note that the chamber size of unknown subsurface voids is not predictable – therefore slope as a proxy for roof thickness is the only insight into ways of predicting collapse. While only one of the two triggers that initiate collapse is observable from the surface, the data to observe that trigger has limited accuracy at this time.

The following scenario will help to demonstrate how the configuration of the cave chamber has a large influence on collapse potential:

A 10 x 2.5 meter void and a 5 x 5 meter void both have an area of 25 square meters, but one of these voids is more prone to collapse than the other. With the same roof thickness (assuming same slope) and everything held constant, the 5 x 5 m void would initiate collapse first due to the greater unsupported span measured as a width

(roof span and roof thickness being the two controls that initiate collapse). As slope decreases over the two voids (the 5 x 5 m chamber having a greater unsupported span) and roof thickness decreases to a point where the roof thickness can no longer support a passage of 5 m, collapse would initiate. The 10 x 2.5 m void would survive a while longer until the roof thickness decreased to an even lesser value that could no longer support a span of 2.5 m.

When evaluating the risk of cave collapse, it is important to over predict rather than under predict the risk. That is, it is better to say, "This area has a risk for collapse" rather than, "It would probably be safe to build there", and then be wrong. The cliché saying – "Better safe than sorry", illustrates this idea rather well.

Geophysical Methods

Gravity surveys have been a successful tool used to located flank margin caves and banana holes in the Bahamas (Kunze and Mylroie, 1991). GPR (ground penetrating radar) was used (William Wilson of Wilson (1995) was hired to do the GPR survey) to locate voids when the San Salvador airport runway was extended from 4000 to 8000 feet (Mylroie, personal comm). Over 25 voids were located and infilled during this project (most likely banana holes) (Mylroie, personal comm). Gravity, while successful, was labor intensive and not amenable to broad reconnaissance (Kunze and Mylroie 1991). The GPR was very successful, but the work was carried out on level, cleared land. In the vegetated, irregular areas, GPR would likely be less successful. It is stated in Kunze and Mylroie (1991) that the dense brush of the Bahamas make GPR impractical. Both GPR and gravity promise methods for determining the location and size of voids and depth, but the use of such tools must be site specific and preferably the site be cleared of the

native bush. When an area is predicted to be at risk for collapse due to the slope of the landscape and the assumption of a large span at depth, it is then that geophysical methods could be used to check for voids beneath the surface.

Future Work

Slope varies depending on where the transect is drawn. Using lidar or advanced satellite data (both capable of sub-meter accuracy) in this study would open up other opportunities to address this problem. The cost for lidar or satellite data far exceeded the budget of this research project; what satellite data was available had worse resolution than the topographic maps (90 m vs 6 m, respectively). Using GIS, the slope could be calculated for an entire study area using the slope tool in spatial analyst. Instead of the slope being calculated over chosen transects, each cell within the raster would have a slope value. The slope calculation in spatial analyst assigns each cell a slope value by taking the maximum change in elevation and dividing it by the distance between the cell and its eight neighbors. The consistency of the GIS slope calculation process removes human error and human bias from the process of slope calculation. With a full sample size of caves, cave maps, and high accuracy elevation data (e.g. Lidar), along with the computing potential of GIS, it is thought that a correlation may be found.

CHAPTER VI

CONCLUSIONS

The purpose of this study was to test the hypothesis that topographic maps produced by the Bahamas Lands and Surveys Department are insufficient in resolution to be used as a predictor of flank margin cave collapse risk in The Bahamas.

Analysis of 107 caves using over 70 topographic map sheets on eight islands shows no clear relationship between derived slopes and cave collapse. The topoographic maps were not sufficient to create a cave collapse prediction model. Even use of slopes derived from six caves with 1 m contour survey produced only a moderate predictive pattern. There is a visually recognizable pattern using the higher accuracy data, especially for pit entrances, but an accurate prediction of collapse cannot be guaranteed. Cave collapse is not only dependent on slope as a proxy for roof thickness but on the configuration of the underlying cave. Flank margin caves are a series of globular chambers with widely varying chamber sizes and roof heights. This cave configuration makes it difficult to determine when any given slope has created a thin roof condition, which would be prone to collapse. Geophysical techniques have promise but are labor intensive, especially in the remote island settings. Flank margin cave collapse is a very complicated problem. It was illustrated in previous literature that flank margin cave collapse was a fairly

straightforward issue, but the use of slope as an indicator for roof collapse is not effective. Slope does demonstrate a relationship with entrance types that are the result of large scale surface erosion (side breach and collapse breach). However, the prediction of those entrances is not possible due to the complexities of the initiation of an entrance. Many things must go into account to predict collapse (roof thickness, chamber size, and chamber configuration). Flank margin caves and banana holes are easy to localize; flank margin caves are under the edges of dune ridges, and banana holes are in late Pleistocene strandplains. However, the specific location of these voids within those localities eludes easy analysis. This study should be used as a guide to evaluate the landscape and consider if geophysical methods are needed for a particular area before development.

REFERENCES

Albury, P., 1975. The Story of the Bahamas. Macmillan Publishers Ltd, 294 p.

Aley, T., 1972, Groundwater contamination from sinkhole dumps: Caves and Karst, v. 14, p. 17–23.

The American Heritage® Dictionary of the English Language, Fourth Edition. 2003. Houghton Mifflin Company. 25 Feb. 2013. www.thefreedictionary.com/collapse

Carew, J.L., Mylroie, J.E., 1995b, Quaternary tectonic stability of the Bahamian Archipelago: evidence from fossil coral reefs and flank margin caves. Quaternary Science Reviews 14: p. 144–153.

Choquette, P.W., and Pray, L.C., 1970, Geologic nomenclature and classification of porosity in sedimentary carbonates. American Association of Petroleum Geologists Bulletin, v. 54, no. 2, p. 207-250.

Doehring, D. O. and Butler J. H., 1974, Hydrogeologic constraints on Yucatan's development. *Science,* v.186, 591-595.

Dreybrodt, W., 2000, Equilibrium chemistry of karst water in limestone terranes, in Klimchouk, A.B., Ford, D.C., Palmer, A.N., and Dreybrodt, W., eds., Speleogenesis—Evolution of karst aquifers: National Speleological Society, Huntsville, AL, p. 126–135.

Ford, D. C., and Williams, P., 2007, Karst hydrogeology and geomorphology. John Wiley & Sons, 562 p.

Ho, C. H., Mylroie, J. E., Infante, L. R., and Rodgers, J. R. III, 2013, Fuzzy-based spatial modeling approach to predict island karst distribution: a conceptual model: Environmental Earth Science, DOI 10.1007/s12665-013-2543-4.

Jenson, J.W., Keel, T.M., Mylroie, J.R., Mylroie, J.E., Stafford, K.W., Taborosi, D., and Wexel, C., 2006, Karst of the Mariana Islands: The interaction of tectonics, glacioeustasy and fresh-water/sea-water mixing in island carbonates: Geological Society of America Special Paper, v. 404, p. 129–138.

Kambesis, P. N, and Machel, H. G., 2013, Caves and Karst of Barbados, In Lace, M. J., and Mylroie, J. E., eds., 2013, Coastal Karst Landforms. Coastal Research Library 5, Springer, Dordrecht, p. 227-244.

Kindler, P., Mylroie J. E., Curran , H. A., Carew, J. L., Gamble, D. W., Rothfus, T. A., Savarese, M., and Sealey, N. E., 2010, Geology of Central Eleuthera, Bahamas: A Field Trip Guide. Gerace Research Centre, San Salvador Bahamas, 74 p.

Klimchouk, A.B. 2007, Hypogene Speleogenesis: Hydrogeological and Morphogenetic Perspective. Special Paper no. 1, National Cave and Karst Research Institute, Carlsbad, NM, 106 p.

Klimchouk, A., Sasowsky, I.. D., Mylroie, J., Engel, S. A., Enegel, A. S., 2014, Hypogene Cave Morphologies, Special Publication 18, Karst Waters Institute, Leeesburg, 103 p.

Knight, F. J., 1971, Geologic problems of urban growth in limestone terrains of Pennsylvania. Bulletin of the Association of Engineering Geologists, v. 8, no. 1, p. 91-101.

Kunze, A. W. G. and Mylroie, J. E., 1991, Use of gravity techniques to detect shallow caves on San Salvador Island, Bahamas. ***In*** Bain, R. J., ed., Proceedings of the 5th Symposium on the Geology of the Bahamas: Bahamian Field Station, Port Charlotte, FL, p 139-149.

Lace, M. J., and Mylroie, J. E., 2013, Coastal Cave and Karst Resource Management. In Lace, M. J., and Mylroie, J. E., eds., 2013, Coastal Karst Landforms. Coastal Research Library 5, Springer, Dordrecht, p. 127-143.

Lascu, I., 2005, Speleogenesis of large flank margin caves of the Bahamas, MSc. Thesis. Department of Geosciences, Mississippi State University, Mississippi State, MS, 218 p.

Meyerhoff, A. A., and Hatten, C. W., 1974, Bahamas salient of North America: Tectonic framework, stratigraphy, and petroleum potential: American Association of Petroleum Geologists Bulletin, v. 58, p. 1201-1239.

Moneymaker, B. C., 1941, Subriver solution cavities in the Tennessee Valley. The Journal of Geology, p. 74-86.

Mylroie, J.E., Ho, H.C., Infante, L.R., Kambesis, P.N., Leist, J.W. in press, Banana holes as syndepositional flank margin caves within an advancing strandplain and their prediction using fuzzy-based spatial modeling. ***In*** Savarese, M. and Glumac, B., eds., Proceedings of the 16th Symposium on the Geology of the Bahamas and Other Carbonate Regions, Gerace Research Centre, San Salvador, Bahamas.

Mylroie J.E., Vacher H.L., 1999, A conceptual view of carbonate island karst. In: Palmer A.N., Palmer M.V., Sasowsky, I.D. eds. Karst modeling. Karst Waters Institute special publication #5, p 48-57.

Mylroie, J.E. and Mylroie, J.R., 2007, Development of the Carbonate Island Karst Model: Journal of Cave and Karst Studies, v. 69, no. 1, p. 59-75.

Mylroie, J.E., 2013, Coastal Karst Development in Carbonate Rocks, In Lace, M. J., and Mylroie, J. E., eds., 2013, Coastal Karst Landforms. Coastal Research Library 5, Springer, Dordrecht, p. 77-110.

Mylroie, J.E. and Carew, J.L., 2013, Field Guide to the Geology and Karst Geomorphology of San Salvador Island, p. 1-89.

Mylroie, J.E. and Mylroie, J.R., 2013a, Caves and Karst of the Bahama Islands, In Lace, M. J., and Mylroie, J. E., eds., 2013, Coastal Karst Landforms. Coastal Research Library 5, Springer, Dordrecht, p. 147-176.

Mylroie, J.E. and Mylroie, J.R., 2013b, Telogenetic Limestones and Island Karst, In Lace, M. J., and Mylroie, J. E., eds., 2013, Coastal Karst Landforms. Coastal Research Library 5, Springer, Dordrecht, p. 375-394.

Mylroie, J.E. Personal communication. Mississippi State University, Feb. 25, 2014.

Palmer, A.N., 1991, Origin and morphology of limestone caves. Geological Society of America Bulletin 103, p. 1–21.

Roth, M. J., 2004, Inventory and geometric analysis of flank margin caves of the Bahamas. MSc. Thesis, Mississippi State University, 117 p. http://sun.library.msstate.edu/ETD-db/theses/available/etd-07062004-164930/unrestricted/monica.pdf

Shackleton, N.J., 2000. The 100,000-year ice-age cycle identified and found to lag temperature, carbon dioxide, and orbital eccentricity: Science, 289, p. 1897-1902.

Uchupi, E., Milliman, J. D., Luyendyk, B. P., Brown, C. O., and Emery, K. O., 1971,Structure and origin of the southeastern Bahamas: American Association of Petroleum Geologists Bulletin, v. 55, p. 687-704.

Vacher, H.L., and Mylroie, J.E., 2002, Eogenetic karst from the perspective of an equivalent porous medium: Carbonates and Evaporites, v. 17, no. 2, p. 182–196.

Waelbroeck, C., Labeyrie, L., Michel, E., Duplessy, J. C., McManus, J. F., Lambeck, K., and Labracherie, M., 2002, Sea-level and deep water temperature changes derived from benthic foraminifera isotopic records. Quaternary Science Reviews, v. 21 no. 1, p. 295-305.

White, W. B., 1988, Geomorphology and hydrology of karst terrains. Volume 464. New York: Oxford university press.

Wilson, W.L., Mylroie, J.E., and Carew, J.L., 1995, Quantitative analysis of caves as a geologic hazard on San Salvador Island, Bahamas, in Proceedings of the 7th Symposium on the Geology of the Bahamas, San Salvador Island, Bahamian Field Station, p. 103–121.

APPENDIX A

TOPOGRAPHIC MAP ANALYSIS DATA

Table A.1 Table showing the slope, entrance type/quantity, and maximum chamber width for each cave used in the topographic map analysis.

OID	Island	Cave Maps	# entrances	Side breach	Collapse breach	Pit breach	Collapse	Chamber size	Hillslope
1	Abaco	8 mile cave	3	0	3	0	y	10	6.8
2	Abaco	Azimuth cave	1	1	0	0	n	18	3.8
3	Abaco	Bellycrawl Cave	1	1	0	0	n	2	6.8
4	Abaco	Bucket Cave	3	1	1	1	y	2	6.8
5	Abaco	Cedar Harbour Cave 1	2	1	1	0	y	7	5.7
6	Abaco	Cedar Harbour Cave 2	2	1	1	0	y	8	5.7
7	Abaco	Cedar Harbour Cave 3	2	1	1	0	y	7	5.7
8	Abaco	Cedar Harbour Cave 4	8	2	6	0	y	10	5.7
9	Abaco	Cedar Harbour Cave 5	5	2	3	0	y	`10	5.7
10	Abaco	Dripping Stones Cave	1	1	0	0	n	5	3.1
11	Abaco	Hole-in-the-Wall Cave	6	0	2	4	y	20	3.8
12	Abaco	Hunter's Cave	1	1	0	0	n	4	11.3
13	Abaco	Little Bay Cave 1	2	2	0	0	n	4	6.3
14	Abaco	Little Bay Cave 2	1	1	0	0	n	12	6.3
15	Abaco	Little Bay Cave 3	1	1	0	0	n	3.5	6.3
16	Abaco	Long Beach Cave	2	0	2	0	y	6	1.3
17	Abaco	Manchineal Cave	3	1	0	2	y	10	3.8
18	Abaco	Sitting Duck Cave	3	1	2	0	y	10	3.8
19	Acklins	Babylon Cave	41	3	0	38	y	24	1.8
20	Acklins	Bloody Hand Cave	3	2	0	1	n	3	7.6
21	Acklins	Dip-N-Break Cave	8	3	0	5	n	12	7.6
22	Acklins	Harbor Cave	6	1	0	5	n	18	11.3
23	Acklins	Jumbey Hole	20	4	0	16	n	36	7.6
24	Acklins	Kinda Big Cave	14	2	2	10	y	15	7.6
25	Acklins	Natural Bridge Cave	2	1	1	0	y	6	7.6
26	Acklins	Nibbles Cave	19	1	1	17	y	12	1.8
27	Acklins	South Bluff Cave	2	2	0	0	n	9	8.0
28	Cat Island	Bluff Cave	2	1	1	0	y	10	5.7
29	Cat Island	Brackish Well	2	0	1	1	y	10	5.7
30	Cat Island	Crown Cave	3	0	1	2	y	12	5.3
31	Cat Island	Industrious Hill	4	4	0	0	n	10	8.1
32	Crooked	1702 Cave	9	2	3	4	y	12	11.3
33	Crooked	Acolyte's Attic	2	1	0	1	n	6	2.9
34	Crooked	Annex A	1	1	0	0	n	10	11.3
35	Crooked	Annex B	1	1	0	0	n	10	11.3
36	Crooked	Black Wall Cave	1	1	0	0	n	6	2.9
37	Crooked	Crossbed Cave	1	1	0	0	n	9	11.3
38	Crooked	Cumulus Cave	1	1	0	0	n	15	11.3
39	Crooked	Fenestral	22	1	0	21	n	9	13.5
40	Crooked	Lowly Cave	1	1	0	0	n	21	11.3
41	Crooked	Owl's Roost Cave	4	2	2	0	y	15	11.3
42	Crooked	Rimout Cave	1	1	0	0	n	21	11.3
43	Crooked	Temple of Athena	6	1	0	5	n	30	2.9
44	Crooked	Winding Bay	1	1	0	0	n	5	13.5
45	Eluthera	Big Blowing Hole	2	1	1	0	y	20	4.8
46	Eluthera	Blow hole	1	1	0	0	n	3	7.1
47	Eluthera	Boiling Hole	1	1	0	0	n	20	9.5
48	Eluthera	Boston Bight	2	2	0	0	n	3	45.0
49	Eluthera	Cow	1	1	0	0	n	2	45.0
50	Eluthera	Crawl thru	3	1	1	1	y	1.5	14.0
51	Eluthera	Dozer	1	1	0	0	n	3	4.8
52	Eluthera	Five Bells	3	1	2	0	y	2	3.6
53	Eluthera	Garden	4	1	0	3	y	13	4.5
54	Eluthera	Hatchet Bay Cave	2	0	2	0	y	40	4.5
55	Eluthera	Laminar Basin	1	1	0	0	n	21	9.5
56	Eluthera	Owl	19	3	3	13	y	13	9.5
57	Eluthera	Reflecting Pond	1	1	0	0	n	3	4.5
58	Eluthera	Safe Harbor	2	1	1	0	y	3	9.5
59	Eluthera	Smoke	1	1	0	0	n	3	5.2
60	Eluthera	Stinging	1	1	0	0	n	2	45.0
61	Eluthera	Ten Bay Cave	26	1	7	18	y	20	2.4
62	Eluthera	The Bull	3	3	0	0	n	3	45.0
63	Eluthera	Wasp Nest	2	1	0	1	n	3	5.2
64	Long Island	BEC Cave #2	1	1	0	0	n	6	25.6
65	Long Island	BEC Cave #3	1	1	0	0	n	14	25.6

Table A.1 (Continued)

OID	Island	Cave Maps	# entrances	Side breach	Collapse breach	Pit breach	Collapse	Chamber size	Hillslope
66	Long Island	Benzie Hill North	2	2	0	0	n	3	14.6
67	Long Island	Benzie Hill South	2	1	1	0	y	3	14.6
68	Long Island	Dutchmans Point	1	1	0	0	n	3	2.3
69	Long Island	Hilldside Grocery	2	0	2	0	y	20	6.8
70	Long Island	Indian Hole Point	3	1	0	2	n	10	9.1
71	Long Island	Lobster	3	0	3	0	y	8	7.6
72	Long Island	Red Roof Cave	3	1	1	1	y	5	5.7
73	Long Island	Salt Pond	6	0	6	0	y	18	5.9
74	Long Island	Salty Dog	1	1	0	0	n	6	7.6
75	Long Island	Stella Maris	1	1	0	0	n	16	17.7
76	Long Island	Termite Mound	1	1	0	0	n	4	4.6
77	Long Island	Walk Through	8	2	6	0	y	10	2.3
78	Long Island	Wasp Pole Cave	1	1	0	0	n	5	6.8
79	New Providence	Bahamas West	2	1	0	1	n	14	4.8
80	New Providence	Bat Cave	4	4	0	0	n	9	4.1
81	New Providence	Caves Point East	3	1	0	2	n	15	5.7
82	New Providence	Caves Point West	1	1	0	0	n	10	5.7
83	New Providence	Clifton Banana Hole	1	0	1	0	y	15	1.1
84	New Providence	Clifton East Cave	4	1	3	0	y	4	2.9
85	New Providence	Harry Oakes	4	2	1	1	y	6	4.4
86	New Providence	Harry Oakes Annex	3	3	0	0	n	4	4.4
87	San Salvador	Altar	1	1	0	0	n	13	2.9
88	San Salvador	Beach	2	1	1	0	y	16	8.5
89	San Salvador	Blowhole	4	0	4	0	y	6	11.3
90	San Salvador	Bug City	1	1	0	0	n	5	17.7
91	San Salvador	Chinese Fire Drill	2	1	1	0	y	1.5	7.6
92	San Salvador	Crescent Top Cave	1	1	0	0	n	4	8.4
93	San Salvador	Dripping Rock	1	1	0	0	n	23	2.9
94	San Salvador	Emerald	1	1	0	0	n	6	17.7
95	San Salvador	Garden	10	0	9	1	y	8	9.1
96	San Salvador	Garden Annex	4	0	2	2	y	11	9.1
97	San Salvador	George Storrs	1	1	0	0	n	17	5.1
98	San Salvador	Granny T	3	0	3	0	y	3	3.0
99	San Salvador	Hurricane	1	1	0	0	n	4	4.6
100	San Salvador	Lighthouse cave	3	0	0	3	n	10	9.5
101	San Salvador	Majors	5	3	0	2	n	10	5.1
102	San Salvador	Midget Horror Hole	1	1	0	0	n	2.5	17.7
103	San Salvador	Old Bottle	4	0	3	1	y	4	9.1
104	San Salvador	Pipe	2	1	1	0	y	NS	8.4
105	San Salvador	Prediction	2	0	2	0	y	2	4.6
106	San Salvador	Reckly Hill Pond Maze	1	1	0	0	n	2	17.7
107	San Salvador	Reckly Hill Pong Water	1	1	0	0	n	10	17.7